FACULDADE DE ENGENHARIA DA UNIVERSIDADE DO PORTO

Storage system for pulsed energy generated by a Pavement Energy Harvesting Solution

Rui da Silva Pinto de Sousa

Mestrado Integrado em Engenharia Eletrotécnica e de Computadores

Institutional Supervisor: Professor Hélder Leite, FEUP

Supervisor: Eng.º, Francisco Duarte, Pavnext

July 23, 2020

Resumo

A crescente preocupação na redução dos combustíveis fósseis como fonte de produção de energia, e a aposta no recurso a fontes renováveis para suprimir a procura de energia eléctrica, está a conduzir ao aparecimento de novas tecnologias capazes de produzir energia eléctrica com um impacto ambiental reduzido.

Com os constantes desenvolvimentos tecnológicos, existe hoje (2020) a possibilidade de desenvolver uma solução de Pavement Energy Harvesting (PEH) que pode recolher energia cinética de veículos e convertê-la em electricidade. A par da geração de energia elétrica, esta tecnologia potencializa a segurança rodoviária através da redução da velocidade do veículo sem qualquer acção do condutor. Aquando da travessia de veículos pelos módulos do sistema PEH, um sistema electromecânico converte o deslocamento vertical da superfície dos módulos em energia eléctrica pulsada. A energia eléctrica produzida requer um sistema de armazenamento para que possa ser utilizada em diversas aplicações eléctricas instaladas localmente.

Este projecto centra-se na modelação e simulação do comportamento de geração eléctrica do módulo do sistema de Pavement Energy Harvesting e o seu armazenamento de energia.

Inicialmente, uma análise comparativa das diferentes tecnologias de armazenamento de energia conduziu à selecção de supercondensadores e ultracondensadores como as soluções mais promissoras para armazenar a energia pulsada do módulo de geração.

Com vista a desenvolver uma solução eficaz e eficiente para o armazenamento de energia pulsada, foi desenvolvido, com recurso à ferramenta MATLAB & Simulink, um modelo representativo do módulo do sistema PEH para simular e avaliar o desempenho de diferentes configurações de sistemas de armazenamento de energia.

A partir da análise dos resultados da simulação, foi possível identificar o sistema híbrido com dois estágios de armazenamento de energia como a configuração mais adequada para armazenar a energia pulsada proveniente do sistema PEH. Esta configuração combina dois módulos de supercondensadores em série como primeiro estágio de armazenamento de energia, e uma célula de ultracondensador como segundo estágio.

Abstract

The increasing concern in the reduction of fossil fuels as an electrical energy generation source, together with the concern in resorting to renewable sources to suppress the electrical energy demand is driving to the appearance of new technologies capable of producing electrical energy with an insignificant environmental impact.

With the constant technological developments, there are nowadays (2020) the possibility of developing a Pavement Energy Harvesting (PEH) solution that can harvest kinetic energy from vehicles and convert it into electricity. Harvesting kinetic energy from vehicles might be increasing road safety by reducing the vehicle speed without any driver action. When vehicles move across the PEH system modules, an electro-mechanical system converts its surface motion into pulsed electric energy. The electric energy produced requires a storage system so it can be used in multiple applications locally installed.

This project focuses on the modelling and simulation of the electric generation behaviour of the PEH module and its energy storage.

At first, a comparative analysis of the different technologies for energy storage has been performed, leading to the selection of supercapacitors and ultracapacitors as the strongest candidates to store pulsed energy from the generation module.

Then a model of the PEH system module is developed based on MATLAB & Simulink to simulate the performance of different energy storage system configurations to achieve an effective and efficient solution.

From the analysis of the simulation results, it was possible to identified the two stage hybrid energy storage system as the most suitable configuration for storing the pulsed energy coming from the PEH system. This configuration combines a two series supercapacitor modules as first energy storage stage and a ultracapacitor cell as second energy storage stage.

Acknowledgments

First of all, I would like to thank to the company Pavnext for the dissertation proposal, specially to Engineer Francisco Duarte for the monitoring during this project.

Secondly, a special thanks to my supervisor Hélder Leite for always being available to help me in overcoming the obstacles faced throughout this project.

I would like to offer my sincere thanks to all those who have contributed, directly or indirectly, to my academic success.

To my parents, I would like to thank for all the opportunities given to me and for the never-ending support. The values you raised me with are the primary reason for coming this far on my academic journey.

To my brothers, I would like to thank for being my closest and most valuable advisors.

A heartfelt thanks to all my friends for always supporting me throughout my academic journey. Especially to my dear friend Miguel Chousal for the incredible companionship throughout the last 3 years.

Rui Sousa

"If you have built castles in the air, your work need not be lost;
that is where they should be. Now put the foundations under them."

Henry David Thoreau

Contents

List of Figures

List of Tables

List of Abbreviations

AC	Alternating Current
CAES	Compressed Air Energy Storage
CTS	Crank to Slider
DC	Direct Current
DG	Distributed Generation
DTCM	Deceleration Tracking Control Mechanism
ECDL	Electrochemical Double Layer
EPR	Equivalent Parallel Resistor
ESR	Equivalent Series Resistor
HEV	Hybrid Electric Vehicle
IW	Inertia wheel
MSCM	Maximum Speed Control Mechanism
PEH	Pavement Energy Harvesting
PHS	Pumped Hydroelectric Storage
PSB	Polysulphide Bromide Battery
RES	Renewable Energy Sources
SC	Supercapacitor
SMES	Superconducting Magnetic Energy Storage
TES	Thermal Energy Storage
UC	Ultracapacitor
VRB	Vanadium Redox Battery

List of Notations

AEPEH	Annual stored energy by the PEH system (kWh)
b_{cb}	Mechanical system clutch bearing friction coefficient
b_{gen}	Generator friction coefficient
DEPEH	Daily stored energy by the PEH system (kWh)
DT	Daily traffic
E	Electric generator armature induced voltage (V)
E_{DC}	Generated energy of each PEH module generator after AC-DC conversion (J)
E_{Gi}	Generated energy of each PEH module generator (J)
EPEH	Total stored energy by the PEH system (kWh)
E_{str}	Stored Energy (J)
E_{strSC}	Stored Energy by the supercapacitor modules (J)
E_{strUC}	Stored Energy by the ultracapacitor cell (J)
ET	Electric torque (N.m)
EVE	Economic value of the PEH system stored energy (€)
F_{SM2}	Force transmitted by the vehicle (N)
g	Gravitational acceleration (m/s^2)
I_{str}	Energy storare system charging current (A)
Jgen	Moment of inertia of the electric generator (kg.m2)
Jiw	Moment of inertia of the inertia wheel (kg.m2)
Jp	Moment of inertia of the mechanical system pinion (kg.m2)
Jsh	Moment of inertia of the mechanical system shaft (kg.m2)
k_b	Electric generator voltage constant
k_t	Electric generator Electric Torque constant
l_m	PEH module width (m)
$l_v w$	Distance between the vehicle front and back wheels (m)
m_v	Vehicle (kg)
N_{mod}	Number of modules of the PEH system
r_p	Mechanical system pinion radius (m)
s_v	Vehicle speed (m/s)
t_1	Time of contact between the vehicle wheel and the PEH module (s)
t_2	Time between the crossing of the front and back vehicle wheels (s)
η_{AC-DC}	Efficiency of the AC-DC conversion system (%)
η_{SC-UC}	Efficiency of ultracapacitor charging process (%)
η_{str}	Efficiency of energy storage system (%)
η_{total}	Efficiency of the PEH module system (%)
$\ddot{\theta}_{gen}$	Generator shaft acceleration (rad/s^2)
$\dot{\theta}_{gen}$	Generator shaft speed (rad/s)

Chapter 1

Introduction

1.1 Context and Motivation

The global increase of the electrical energy consumption, and the urgent environmental concern in reducing pollutant emissions, are driving the development and implementation of cleaner alternative generation technologies. Within this context a Pavement Energy Harvesting (PEH) system capable of harvesting the vehicles mechanical energy from the road pavements and convert it into useful electrical energy has been developed.

The PEH system is composed of several modules that can be defined as kinetic bumps. When the vehicle crosses over the PEH system, each module converts its surface vertical displacement into angular displacement of two generators shafts, through a mechanical system. The generators are then responsible for converting the mechanical energy into electrical energy.

Like the majority of renewable energy sources technologies, PEH system does not allow electrical energy to be produced when it is needed, but only when the resources are available. In order to become a fully effective electrical energy generation technology, the PEH system requires an energy storage system. This way the energy generated by the PEH system can be stored and used when its needed in several applications on sight.

Since the energy generation depends on the frequency of the vehicles crossing the PEH system, it is required a energy storage system capable of storing the pulsed energy coming from each module.

1.2 Methodology

This project focuses on the development of an energy storage system capable of storing pulsed energy generated by the PEH system.

To accomplish this, firstly, a close examination of the available energy storage technologies is conducted to chose potential storage solutions.

Subsequently, a simulation tool, using MATLAB & Simulink was developed to evaluate the energetic performance of the PEH system with different energy storage configurations.

The simulation tool allows the simulation of each developed configuration in a expeditious way.

Finally, through the comparison of the simulation results it is possible to chose which energy storage configuration presents the most effective and efficient performance.

1.3 Structure of the dissertation

This dissertation is organized into 6 chapters.

Chapter 1 comprises the introduction to the dissertation, the context in which the project is placed, the motivation and the structural organization of the dissertation.

Chapter 2 presents an introduction to the PEH system for which a storage system is to be developed. A succinct explanation of the PEH system module electro-mechanical system demonstrates the generation of pulsed energy.

In Chapter 3 is presented the state-of-the-art of the existing electrical energy storage technologies. A comparison between the described technologies allows to conclude which one is the most compatible with the requirements of the PEH system, and therefore the most feasible to be implemented.

Chapter 4 presents the modelling and simulation of the PEH module with several possible configurations of the energy storage system. A simulation tool, developed using MATLAB & Simulink, allows the evaluation of its performance in terms of energy generation and storage using different configurations. At last, the finest energy storage system solution is chosen to be implemented.

In Chapter 5 a technical and economic study is carried out regarding the applicability of a complete PEH system, with a total of ten modules. It is presented the expected stored energy in a period of one year, as well as a critical reflection on the economic potential of the technology implementation.

Chapter 6 presents the main conclusions drawn throughout the development of this dissertation. This chapter ends with a reference about the potential future work to be done on this topic that can lead to more effective results

Chapter 2

Pavement Energy Harvesting System

2.1 Introduction

In the present energetic paradigm (year 2020) most electrical energy demand is still suppressed by electrical energy production that uses non-renewable resources, making economies dependent on fuel costs and leading to dangerous environmental damages. The efforts on the energy sector are focused on changing this paradigm, by decentralizing energy production and making it closer to the point of consumption, resorting to renewable resources [1].

Other than the major energy sources in the renewable energy sector, such as hydro, solar and wind, energy harvesting systems are beginning to be adopted in locations where it is possible to generate electrical energy from small energy variations such as thermal gradients, pressure, vibrations, radiofrequency or electromagnetic radiation, among others [2].

Energy harvesting consists in a system using interfaces, storage devices and other units to capture, convert and utilize energy [2][3]. In short, an energy harvesting system purpose is to convert renewable energy into other useful types of energy, including electricity[4].

Considering the implementation of an energy harvesting system on pavements, the technologies that use solar radiation and the ones that use mechanical energy from vehicles loads have great potential, since road surfaces are continuously exposed to these two phenomena.

In [1], a study of energy harvesting on road pavements state-of-the-art was carried through, focusing on the development of energy harvesting technologies for road pavement. This research describes and compares the technologies that are being studied and developed. It concludes that, presently, most research and development is being performed on the technologies that make use of vehicle mechanical energy, specifically on electro-mechanical systems, that harvest vehicle mechanical energy and generates electrical energy using electromagnetic generators. These, combined with hydraulic systems, have registered the highest energy generation values in experimental tests, higher potential in terms of energy conversion efficiency, and adaptability to road pavement technologies.

In this chapter, an explanation of the electro-mechanical system of the Pavement Energy Harvesting (PEH) in study is presented in order to understand its mechanical and electrical behaviour,

hence its energy storage requirements.

2.2 Electro-mechanical system

As Figure 2.1 shows, the PEH system consists in a group of modules, up to a extension of 20 meters, embedded in the road pavement capable of harvest kinetic energy from vehicles and convert it into electricity. An electro-mechanical system was developed to make this conversion possible.

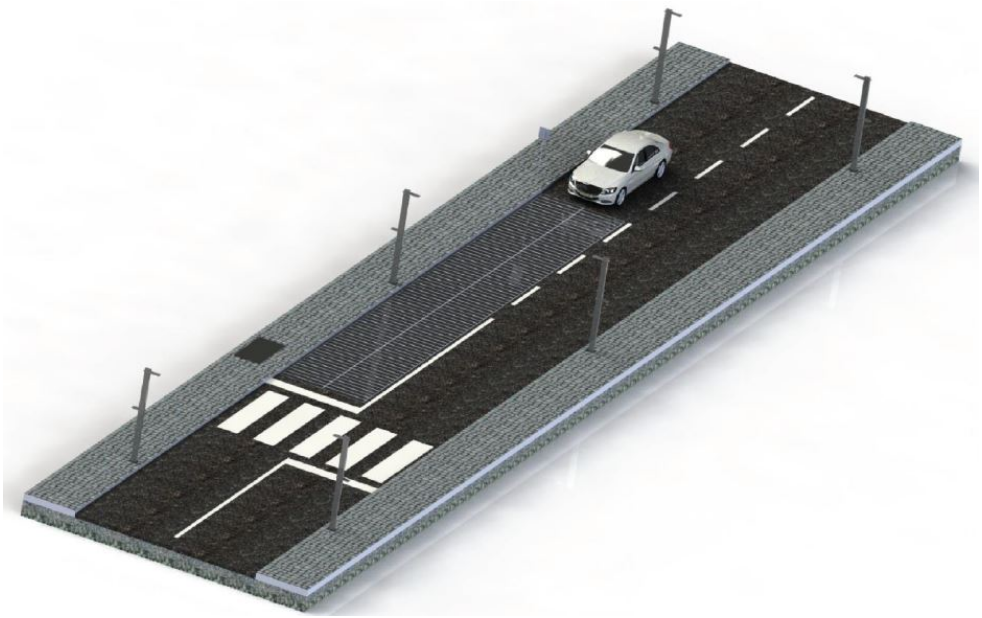

Figure 2.1: 3D module of the expected final PEH system, source [5]

The electro-mechanical system in each module of the PEH system is responsible for converting the vertical displacement of the module surface into angular shaft displacement. Simplified, a module is composed of: (i) an optimized surface to harvest the vehicle's kinetic energy, (ii) a mechanical system to transform the amplitude and direction of the delivered force and (iii) two electromagnetic generators.

2.2.1 Mechanical system

In [5] different road pavement energy harvesting devices using electro-mechanical systems were studied to come to conclusions about their efficiencies. The study aims to know the most efficient solution in converting the linear motion of the PEH module surface into a rotational motion of an inertia wheel (IW) that is connected to the electromagnetic generators shafts.

A new mechanical system was presented to maximize the rotation of the generator shaft by maximizing the amount of force transmitted from the surface with the maximum possible displacement. This new mechanical system, presented in Figure 2.2, called a crank to slider (CTS),

uses a crank connected between the module surface and a slider, combining the maximization of both the transmitted force and shaft rotation.

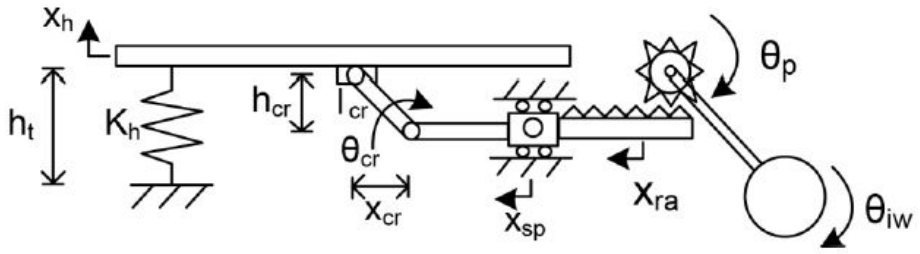

Figure 2.2: PEH module's CTS mechanical system presented, source [5]

When a vehicle moves across the module, the module surface has a linear displacement actuating the crank with a rotational motion, depending on its length and initial angle. The crank actuates the slider, which is connected to a rack. Then, the rack actuates a pinion with a rotation motion. The pinion is connected to an IW which is connected to the electric generator shaft. The system also includes a spring that returns the surface to its initial position.

2.2.2 Electrical system

The PEH module uses two permanent-magnet alternating-current (AC) synchronous generators to convert the mechanical energy delivered by the mechanical system into electrical energy. The mechanical system torque arouses the generator shaft with a rotational speed, defined by the IW, resulting in the development of an electromagnetic force, which represents the generator armature induced voltage. In a permanent-magnet AC synchronous generator the electromagnetic force , depends on the generator shaft rotational speed.

Since the generators produce AC current, power electronics are then used to adapt the generated current to direct-current (DC) allowing the storage of the produced energy.

2.3 Final Remarks

The PEH module electro-mechanical system makes it possible to harvest the vehicles kinetic energy and to convert it into electricity as well as reducing the vehicles speed.

The new mechanical system presented in [5] applied on the PEH system module grants an increase of the transmitted force when compared with other systems, leading to a higher mechanical energy transmission inducing a greater acceleration of the IW and consequently a greater acceleration of the generator shaft. The greater acceleration of the generator shaft renders a higher rotation speed and a higher amount of energy transmission, delivery and conversion.

Since the generators in the module produce energy when a vehicle moves across it, the generated energy is depending on the frequency of the local road traffic and comes in the form of pulsed energy, which requires a storage system capable of fast charging and with a high power density.

Chapter 3

Electrical Energy Storage: State-of-the-art

3.1 Introduction

In today's world there is an increasing global need for energy with the requirement of being cleaner than the energy produced from the traditional generation technologies. This need has promoted the penetration of distributed generation (DG) technologies and, primarily, of renewable energy sources (RES). The inherent intermittency of supply from such technologies makes them not as reliable and as easy to adjust to changing demands cycles as the output of the traditional generation technologies, making energy storage the key to unlock the door of renewable energy.

It is natural to expect that storage will play an important role in electricity networks providing the reliability needed for RES act as primary sources of energy. Energy storage technologies present several advantages that results in improving the energy supply control from RES.

With the wide energy requirements of an energy storage, great progress has been achieved in the development of these technologies giving rise to a wide variety of devices. Howbeit there is no technology able to fulfill both high energy and high power requirements.

This chapter aims to review the electrical energy storage technologies with specially emphasis on batteries and supercapacitors which are the strongest candidates to be implemented in the energy storage of the Pavement Energy Harvesting (PEH) system.

3.2 Classification of the Electrical Energy Storage technologies

The existing, and in development, energy storage technologies can be classified by two main criteria, function and form. In concern of function, energy storage technologies can be divided into those presenting high power ratings and small energy density, and those capable of supplying energy for longer periods of time with higher energy density, but lower power ratings[6]. For storing the pulsed energy coming from the PEH system, power and energy density are the main performance metrics to consider. Power density is the power that can be derived per unit weight

or volume of the cell. Energy density is the energy that can be derived per unit volume or weight of the cell [7].

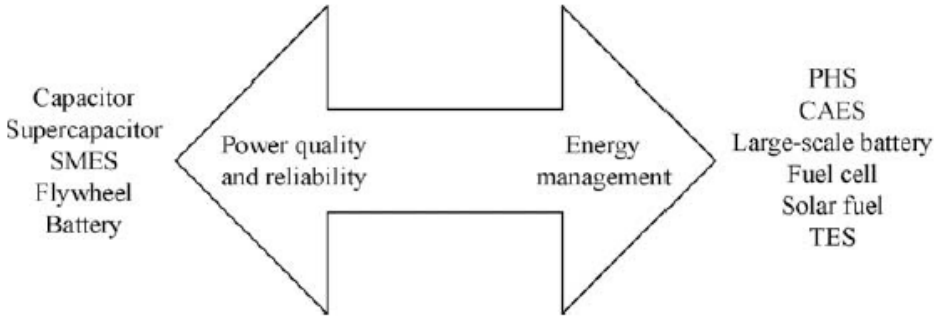

Figure 3.1: Energy storage classification regarding function, source [6]

The energy storage technologies can be classified by the form of storage into the following: mechanical energy storage, chemical energy storage, electro-chemical energy storage, electrical energy storage and thermal energy storage [6].

3.3 Mechanical Energy Storage

The most popular mechanical energy storage technologies are pumped hydroelectric storage (PHS), compressed air energy storage (CAES) and flywheels. Although the applications differ from each one of these technologies, all of them store electrical energy in form of mechanical energy.

3.3.1 Pumped hydroelectric storage (PHS)

Pumped hydroelectric storage (PHS), depicted in Figure 3.2, is the method through which electricity is stored and generated to meet high peak demands by moving water between reservoirs at different elevations. When in charging mode, during to off-peak hours, the water is pumped from the lower to the upper reservoir, storing electricity in form of hydraulic potential energy. In discharging mode, during peak hours, the water flows to the lower elevation reservoir, driving the reversible turbines and converting the potential energy into electricity. The amount of energy stored is proportional to the difference in heights between the two reservoirs and the volume of water stored.

PHS is a mature technology widely deployed, with high durability and long storage period. Taking into account evaporation losses from the exposed water surface and conversion losses, approximately 70-85% of the electrical energy used to pump the water into elevated reservoir can be regained [8].

The PHS rating is the highest among the electrical energy storage technologies available, consequently it is generally applied for energy management, frequency control and provision of reserve [6].

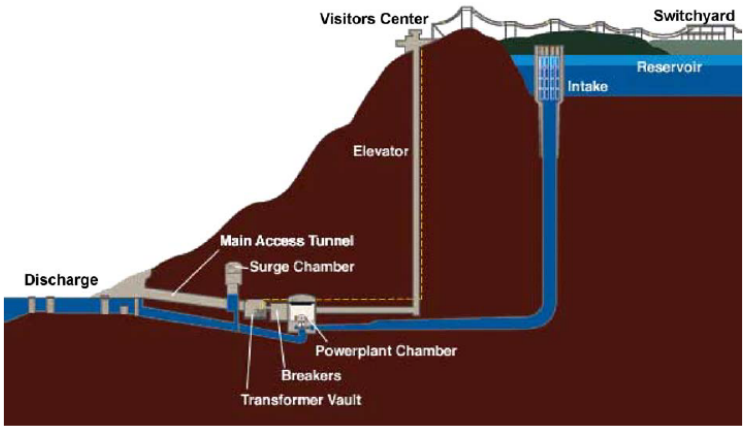

Figure 3.2: Typical PHS plant , source [11]

3.3.2 Compressed air energy storage

Compressed air energy storage (CAES) operates based on conventional gas turbine generation. It decouples a conventional turbine gas compression and expansion cycles into two distinct processes and stores the energy in the form of compressed air elastic potential energy.

The charging process occurs during low demand with compressing air into reservoirs, which may be natural or artificial caves. Compressed air is then drawn from the storage reservoir when the process is reversed, it is heated and expanded via a high pressure turbine. Both high and low pressure turbines drive a generator producing electricity. The waste heat of the exhaust can be captured via a recuperator before being released, and can be reused to increase the discharge efficiency [6][9].

The CAES system presents high durability, however, similar to PHS, the implementation of the CAES relies on favourable geographical location and it is only attainable for power plants that have nearby rock mines, salt caverns, aquifers or depleted gas fields.

To overpower this drawback, some improved CAES systems are suggested or under investigation, including the Small-Scale CAES with Thermal Energy Storage (TES) [10][9]. The conventional type of systems heve been used for a large-scale storage and there are only a few installations worldwide. Figure 3.3 depicts a schematic diagram of CAES.

3.3.3 Flywheel

Flywheels store energy mechanically in the form of kinetic energy in the angular momentum of a spinning mass. During charge a motor accelerates the flywheel, and once it starts rotating

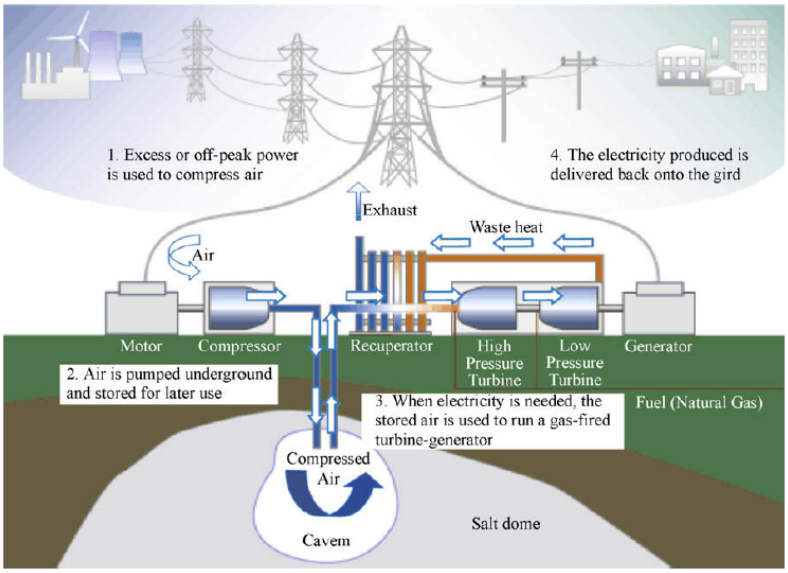

Figure 3.3: Schematic diagram of CAES , source [6]

it becomes a mechanical battery with a certain amount of energy. The total stored energy of a flywheel depends on the size, speed of the rotor, and consequently of its moment of inertia. During discharge the stored energy is withdrawn through slowing down the flywheel and returning the kinetic energy to the motor, which operates in generator mode. Figure 3.4 shows the mains components of a typical flywheel system.

There are two types of flywheels: they can be either low-speed or high-speed, also designated high-power and high-energy respectively. The low-speed flywheel, typically with metal rotor and conventional bearings, has a short discharge time (some seconds to a few minutes). Conversely high speed flywheels use advanced composite materials for the rotor with ultra-low friction bearings assemblies, being able to come up to speed in a shorter period of time and to supply energy for longer time periods. Even though high-speed flywheels show a better energy performance, this technology is about 100 times more expensive than the low-speed flywheels.

The flywheel stands out among the various energy storage technologies by its high cycling capability, being able to perform several hundreds of thousands of full charge-discharge cycles and presenting high charge and discharge speeds, as well as presentig high power rating. Besides that, typically flywheels present a high efficiency, in the range of 90-95%. The main disadvantages of flywheels are the high acquisition cost, specially with the high-speed flywheels, and high self-discharge rates which promotes the deterioration of the energy efficiency when cycling is not continuous. Other important drawback is the flywheel lifetime, quoted around 20 years which constitutes a limiting factor in some applications.

This technology has been successfully deployed enabling the growth of RES penetration in remote electric systems [6][11][8].

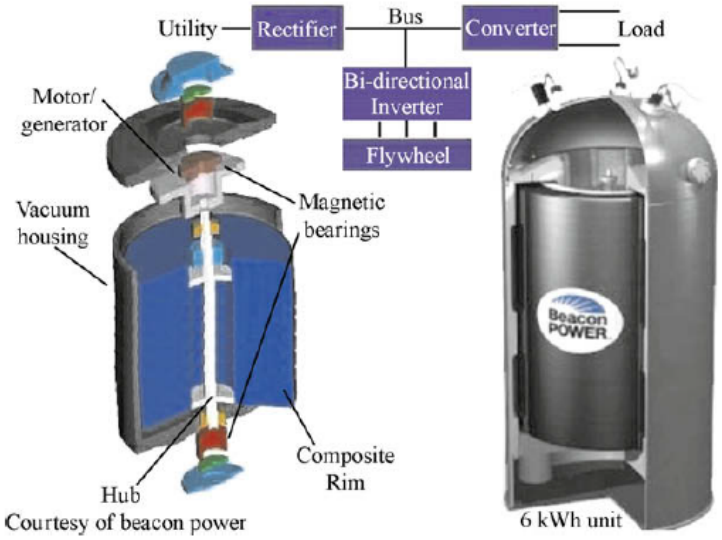

Figure 3.4: Flywheel system , source [6]

3.3.4 Chemical Energy Storage

As the name suggests chemical energy storage technologies store electrical energy in form of chemical energy. The most promising technologies regarding chemical energy storage employ Hydrogen, being one of the most cost efficient storage solutions and presenting low levels, or even none, of pollutants emissions.

3.3.4.1 Hydrogen storage systems (with fuel cells)

These storage systems use hydrogen as a medium to store electricity. The energy is firstly stored via producing hydrogen, which is stored and supplied to a fuel cell that uses it to produce electricity.

It is possible to obtain hydrogen through its extraction from fossil fuels by reacting steam with methane or through the use of electricity electrolysis. The electrolysis is the process that allows electricity to be stored in a direct way. This is a promising technique since it is the most efficient and represents a non pollutant procedure.

Pressured vaporous hydrogen, cold liquid hydrogen or hydrogen compound in chemical or physical structures are the three techniques that can be used with storing hydrogen, being the last mentioned the most suitable for portable and space relevant applications [8].

3.4 Electro-chemical Energy Storage

Electro-chemical energy storage refers to batteries. Batteries are eletro-chemical cells that store energy in the form of chemical energy where electro-chemical reactions take place once it is connected to an electronic load.

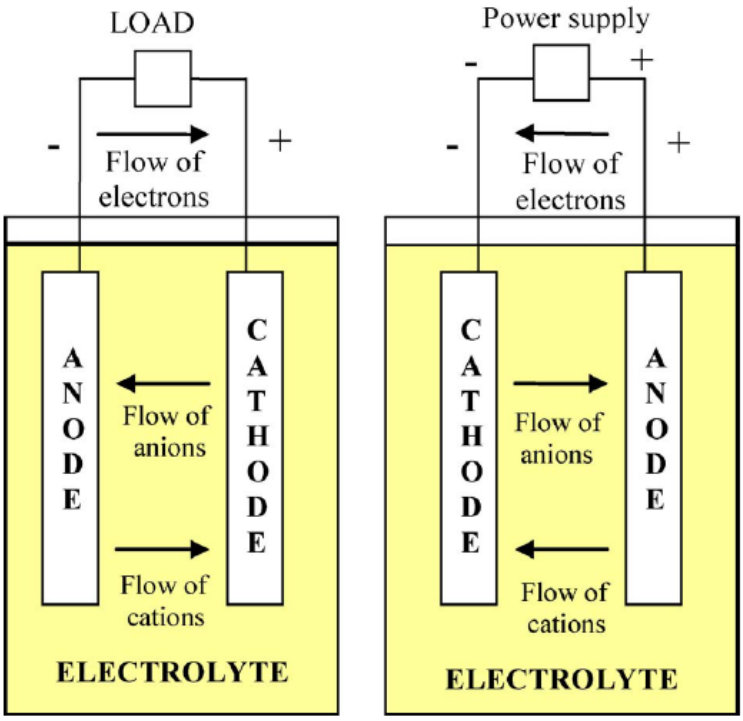

Figure 3.5: Electro-chemical cell diagram , source [11]

Batteries can be one of two existing types, primary or secondary batteries. Primary batteries can only be used once to generate electricity, thus they can not be recharged. Oppositely, in secondary batteries when current is applied at a potential higher than the cell potential, the reverse redox reaction occurs enabling charging. By these means, secondary batteries can be used reversibly for many times [12].

The inability of recharging of primary batteries makes them not suitable to implement in this project, thus this analysis will focus exclusively in secondary batteries.

A rechargeable battery incorporates one or multiple electro-chemical cells, connected in series, parallel or both depending on the desired output voltage and power. As illustrated in Figure 3.5, each cell comprises the positive electrode (cathode) and the negative electrode (anode), both being immersed in a liquid or solid electrolyte producing a cell voltage, and separators between positive and negative electrodes that provide electrical insulation [11].

During discharge, electro-chemical reduction-oxidation reactions occur at the two electrodes, generating a flow of electrons through an external circuit from the cathode to the anode. As aforementioned, the reactions are reversible, enabling the battery to be recharged by applying an external voltage across the electrodes. With the use of different electrodes and electrolytes there are a panoply of batteries suitable to operate in different conditions and applications. The depth of discharge directly influences the durability of the batteries enhancing the importance of this criteria when evaluating different technologies [8].

Batteries present several advantages, such as, fuel flexibility and environmental benefits, rapid

response to load changes enhancing the system stability,modularity and portability. Batteries normally present low standby losses and cab have high energy efficiency (60-95%) [6].

3.4.1 Lead-acid battery

Lead acid batteries were invented in 1859 and are the oldest and most widely use secondary batteries. In the charged state a lead acid battery is comprised of lead metal and lead oxide electrodes immersed in a electrolyte of about 37% sulphuric acid. In the discharged state both electrodes become lead sulphate and the electrolyte turns into mostly water. The two most extensively used types of lead acid batteries are the flooded battery, that requires regular topping up with distilled water, and the sealed maintenance free battery [6].

Lead acid battery presents low cost and a high reliability and efficiency, however its application has been very limited due to its poor low temperature performance (requiring a thermal management system), low energy density, and its short cycle life [6][8]. Attempts to fully discharge a lead-acid battery can be particularly damaging to the electrodes thus drastically harming the lifetime of the device [11].

Lead acid batteries main application has been in vehicle motors. This type of battery controls the starting, lighting and ignition, thus being called SLI batteries, making it a mature technology for all the experience gathered from decades of use in the vehicle industry. Nevertheless, lead acid batteries have also been used in a few large-scale commercial energy management systems [12][7].

3.4.2 Nickel-cadmium battery

Nickel cadmium batteries (NiCd) consist on a nickel hydroxide positive electrode plate, a cadmium hydroxide negative electrode plate, a separator and an alkaline electrolyte. The cathode and the anode plates are isolated from each other by the separator and rolled in a spiral shape inside a metal sealed case equipped with a self-sealing safety valve.

NiCd batteries are a mature and popular technology offering advantages like robustness to deep discharges, a long cycle life and temperature tolerance. The key feature of NiCd batteries when compared to lead acid batteries is the higher energy density, having by this mean, the edge over this technology. These features make NiCd batteries suitable at appliance level. However these batteries also present some heavily drawbacks, such as, the use of cadmium, a highly toxic material, relatively high cost due to expensive manufacture, the mandatory perform of a periodic complete cycle and the need for advanced monitoring during charge and discharge, due to memory effect [6][8]. The memory effect means that the voltage at which discharge ceased is the same that will be attained when charging instead of the maximum voltage possible [12].

In Europe the use of NiCd batteries for consumer appliances has been banned by the Directive 2006/66/EC [8], however NiCd batteries are commercially used for industrial UPS applications such as in large energy for renewable energy systems [11].

3.4.3 Nickel-metal hydride battery

Nickel-metal hydride battery (NiMH) batteries are much the same as NiCd with the major difference of NiMH type using hydrogen-absorbing alloy for negative electrode instead of cadmium. The use of non-toxic materials makes NiMH batteries more environmentally friendly. In addition to that, this type of battery show a high energy density, nearly the double of the energy density of NiCd. However, NiMH batteries are in general less durable then NiCd batteries and can suffer from high self discharge, as well as poor cycling ability and lower shelf-life at higher ambient temperatures. The memory effect on NiMH battery is similar to the one experienced in NiCd battery.

NiMH battery replaced NiCd in most applications in consumer electronics, mobile computing and wireless communication and processing as a result of its better energy density performance. It is available up to the kW scale being used in hybrid electric vehicle (HEV) and electric vehicles applications [12][8][7].

3.4.4 Sodium-sulfur battery

Sodium-sulfur (NaS) battery is a high temperature battery, with a working temperature in the region of 300-350^{o}C, that consists of liquid sulphur at the positive electrode and liquid sodium at the negative electrode as active materials separated by a solid ceramic electrolyte [6].

NaS batteries advantages comprise high efficiency, pulse power capability over six times their continuous power rating, low maintenance, and good scale production potential. These attributes make NaS batteries suitable to be economically used in combined power quality and peak shaving applications [6][8].

In terms of disadvantages, NaS batteries require a heat source to operate at a high temperature which uses the battery's own stored energy. Moreover, the highly corrosive nature of sodium brings corrosion problems to this technology that may diminish its reliability [11].

3.4.5 Sodium nickel-chloride or ZEBRA battery

Sodium-nickel chloride (Na-Ni-Cl) battery, also referred as ZEBRA battery, uses nickel chloride as its positive electrode. ZEBRA batteries have a fast response robustness to full discharge and a very high energy density. Compared to NaS batteries, this technology has potentially better safety characteristics and a higher cell voltage. In terms of its applications, ZEBRA batteries are favored by being small and light cells. The main drawbacks of ZEBRA technology focus on its high cost and high self discharge. This technology has been widely deployed in electric vehicles and submarines and it is expected a great potential for these devices in renewable energy applications [13][8].

3.4.6 Lithium ion battery

Lithium ion (Li-ion) battery has a lithiated metal oxide cathode, a graphitic carbon with a layering structure anode and the electrolyte consists of lithium salts dissolved in organic carbonates. When charged, the lithium atoms in the cathode become ions and flow through the electrolyte to the carbon anode combining with external electrons and are deposited between the carbon layers as lithium atoms [6].

The Li-ion battery is temperature dependent which implicates that high temperatures quickens its aging. Moreover, these batteries also require a built in circuit to limit the peak voltage of each cell during charge and to prevent the cell voltage from dropping too low in discharge. The battery lifetime can be heavily shortened due to deep discharges [11].

In the other hand, these batteries present high reliability and efficiency, good energy density, slow self discharge rate and long lasting lifetime[8]. Furthermore, the small size and low weight of the Li-ion system makes it ideally suitable to portable applications. They are however still costly for medium and large-scale power applications. Most of the research and development heads toward reducing the capital cost of these batteries through the optimisation of ancillary components such as packaging and the charge/discharge voltage control circuit [14]. The cost reduction aims to capture large new energy markets like clean-energy storage and electrical vehicles [7].

3.4.7 Flow batteries

Differently from conventional batteries, flow batteries use electrolyte solutions in external tanks to store energy. A reversible electro-chemical reaction between the two electrolytes takes place at the electrodes allowing the release of energy. The capacity of the system is determined by the size of the electrolyte tank and the power rating is independent from the former one and is determined by the size of the cell stacks. These features grant independent scaling of power and energy capacities.

These systems present advantages such as high flexibility in terms of energy, high efficiency, short response times, symmetrical charge and discharge and quick cycle inversion. Moreover, flow batteries can be optimised for either active or reactive power. Conversely, flow batteries present low power density, use some toxic materials and show insufficient deployment at commercial level. Another major drawback of the flow-battery system is the aggravated capital and running costs related to the operation of what is, in effect, a chemical plant involving pump systems and flow control with external storage [8][6][14].

There are three major leading designs of flow batteries: vanadium redox (VRB), zinc Bromide (ZnBr) and Polysulphide bromide battery (PSB) [14], with VRB and ZnBr batteries being the ones available on the market [8].

3.4.8 Metal-air batteries

A metal-air battery uses metal as a fuel to supply electricity and is composed of a metal anode, an air (oxygen) cathode and an electrolyte through which ions can diffuse and oxidize the anode

[12]. Commonly available metals with a high energy density, such as aluminium or zinc, are used as anodes in metal-air systems, while the cathodes, or air electrodes, can be made of porous carbon structure or of a metal mesh covered with proper catalysts [6].

Metal-air batteries are very compact and inexpensive systems and potentially have the highest energy density, with the additional advantage of having a reduced environmental impact with the use of non-toxic and recyclable materials [8]. The major drawback in metal-air batteries is the difficulty of electrical recharge and the need of material replacement, thus the therm mechanically rechargeable batteries [12]. Therefore metal-air batteries, although promising, are not yet ready for electrical energy storage [7].

3.5 Electrical Energy Storage

3.5.1 Superconducting magnetic energy storage (SMES)

SMES stores electric energy in a magnetic field created by the flow of direct current in a superconducting coil. A typical SMES system, depicted in Figure 3.6, consists of three major components: a superconducting unit, a cryostat system (a cryogenic refrigerator and a vacuum-insulated vessel) that ensures the superconducting state of the inductor, and a power conversion system [6].

The superconducting material of the coil offers no resistance to the electron flow, thus the SMES system presents high energy storage efficiency since energy losses are effectively zero [14]. Moreover, SMES exhibits high durability and reliability since the superconducting coil does not degrade with usage or time. These two features are only dependent of ancillary equipment, such as the power conversion system. Furthermore, SMES also has a short-response time and requires no maintenance. The major drawbacks are the very high cost and the impact of the magnetic field [8].

SMES systems are appropriated to be used in solving voltage stability and power quality problems for large industrial costumers and for short-duration small-sized applications [8][6].

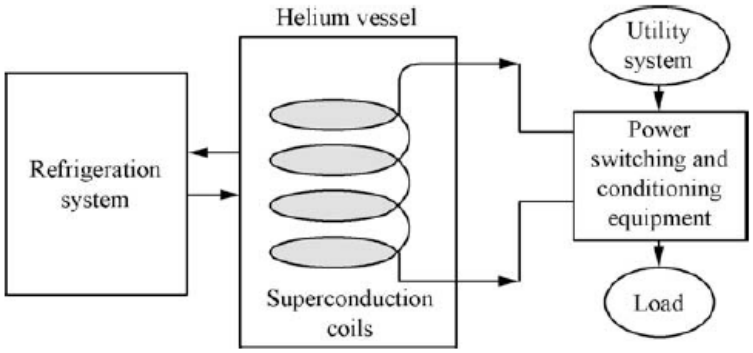

Figure 3.6: SMES system diagram, source [6]

3.5.2 Capacitors

A capacitor is composed by two metal plates separated by a nonconducting layer called a dielectric. While one plate is charged with electricity from a direct current source, the other plate has a charge of opposite sign induced in it. Capacitors exhibit impressive performance in charge/discharge cycles since these processes are substantially faster than conventional batteries. This feature allows capacitors to be cycled tens of thousand of times with a high efficiency. Capacitors have been deployed for peak load summer for less than 1h with small capacities. Conventional capacitors present low energy density requiring a sizeable area of the dielectric in case of need of a larger capacity, making the use of large capacitors uneconomical and unwieldy. In order to achieve greater capacitance , supercapacitors have been developed [6]. This technology will be discussed below.

3.5.3 Supercapacitors

Supercapacitors offer much greater capacitance and energy density than conventional capacitors in compact designs [6]. Supercapacitors, like conventional capacitors, store energy by means of static charge rather than an electro-chemical process inherent to the battery, and can offer much greater capacitance thus enhancing energy density [8]. This storage technology currently fills the gap between batteries and conventional capacitors. Although, supercapacitors can store thousands of times more charge than conventional capacitors, they still present lower energy density when compared to batteries [15].

Figure 3.7 illustrates the supercapacitor taxonomy. Depending on the storage mechanism or cell configuration, supercapacitors can be categorized into electric double layer capacitors (EDLC), pseudo-capacitors and hybrid capacitors [11].

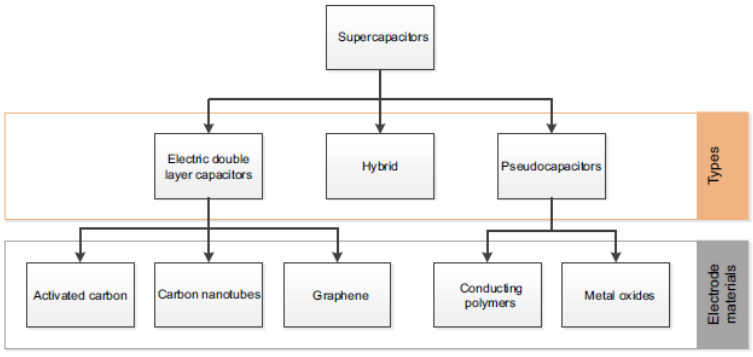

Figure 3.7: Supercapacitors taxonomy , source [16]

EDLCs use high specific-surface area nanoporous materials as active electrode, in order to obtain huge capacitance in comparison with conventional capacitors [16]. As depicted in Fig 3.8, EDLCs have a double layer construction usually consisting of nanoporous active carbon, immersed in liquid electrolyte.

Contrarily to batteries, EDLCs do not make use of chemical processes during charge depending only on electrostatic action being easy to reverse the effect with minimal degradation in deep discharges or overcharge, extending the device cycle life . Moreover, the non-existence of chemical reactions allows EDLC to be quickly and easily charged and discharge. Therefore, supercapacitors present high energy efficiency [11].

The majors drawbacks of EDLCs are the much higher terminal voltage variation and the higher self-discharge rate when compared to typical batteries [7][15]. EDLCs are the most common type of supercapacitor and the least costly to manufacture [11].

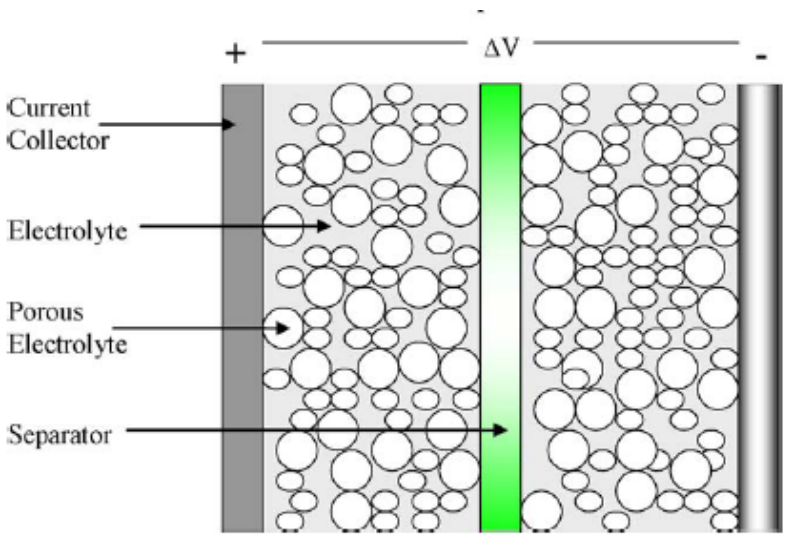

Figure 3.8: EDLC cell structure , source [11]

Pseudo-capacitors consist of metal oxides or conducting polymers as electrode, combining electrostatic and pseudo-capacitive charge storage mechanisms. The charge storage mechanism of pseudo-capaitors relies on fast redox reactions occurring on the electrode surface and the use of such electrodes enables pseudo-capacitors to hold much higher specif capacitance values compared to EDLC. Since redox reactions are used, similar to batteries, pseudo capacitors can suffer from poor mechanical stability and consequently lower life cycle [16][15]. Moreover, pseudo-capacitors are still very expensive to produce and present lower efficiencies and lower voltage potential [11].

Hybrid capacitors stand out by the ability of reaching higher energy densities than the other supercapacitors without prejudice for cyclic stability or affordability [11]. The technology consists of combining an capacitive or pseudo-capacitive electrode and a battery type electrode thus benefiting from both the capacitor and the battery properties. Currently there are two different approaches to hybrid systems, pseudo-capacitive metal oxides with a capacitive electrode carbon electrode, and lithium-insertion electrodes with a capacitive carbon electrode. The emerging developments in the area of Li-ion batteries makes the Li-ion capacitors (LiCs) a promising electrical energy storage technology [15].

LiCs present about four times more energy density when compared do EDLCs. Additionally, compared to EDLCs, LiCs have lower initial self-discharge rate [17]. Due to its superior performance when compared to other supercapacitors, from now on LiCs are referred as ultracapacitors. These features make ultracapacitors fill the gap between Li-ion batteries and EDLCs [15].

The high power storage ability together with fast charge and discharge cycles, make all supercapacitors suitable for applications in which power bursts are needed. Recovery systems, like regenerative braking, short duration peak power boost and short term power back up for UPS systems, are some of the main applications of supercapacitors. Supercapacitors can also be combined with a battery based UPS system, creating what is called a hybrid storage system. This coupling allows load sharing between the battery and the supercapacitor and this way the power and energy characteristics of the storage system are decoupled enabling the use of smaller batteries and enlarging its life time [16][11].

3.6 Thermal energy storage (TES)

Thermal energy storage (TES) systems store electricity as heat, at low or high temperatures, so that when needed, it can be converted back into electricity using heat engine cycles. The energy input of a TES system can be provided by electrical resistance heating or refrigeration/cryogenic procedures. On that account, the overall round trip efficiency of TES is low and the high cycle life efficiency could be higher. Even with low efficiencies TES systems exist in a wide spectrum of applications essentially for being benign to the environment and for presenting particular advantages for renewable and commercial buildings.

TES systems are classified depending on the operating temperature of the energy storage material in relation with the system location temperature. Two TES systems can be distinguished, the low temperature TES and high-temperature TES [8][6].

3.7 Comparison of electrical energy storage technologies

This Section focuses on the comparison of the technologies described above in order to find the ones which characteristics best suit the requirements of this project.

First and foremost, the storage technologies that present notorious hindrances to be applied on this project are eliminated from the contest of best suitable technology for storing pulsed energy. PHS and CAES, rely on favourable geographical location which is impossible to grant in a PEH application. Hydrogen storage systems and flow batteries use tanks to store hydrogen and electrolyte solutions respectively, which can lead to sizing problems. Metal-air batteries are mechanically rechargeable and for that reason not suitable to the project. At last, TES systems exhibits low efficiency and it will not be considered as a possible solution.

Table 3.1 compares the main features of the technologies considered to be implemented in this project.

Table 3.1: Comparison of electrical energy storage technologies

	Storage technologies								
	Lead-acid	Ni-Cd	NiMH	Li-ion	NaS	Zebra	Flywheels	SMES	Supercapacitors
Power rating (MW)	0.001-50	0-46	0.01 to MW	0.1-50	0.05-34	0.001-1	0.002-20	0.01-10	0.001-10
Discharge duration (h)	h	s-h	s-h	0.1-5	5-8	min-8	s-15min s	s	s
Energy density (Wh/kg)	30-50	50-75	30-110	75-250	150-240	100-140	5-130	0.5-5	0.05-30
Power density (W/kg)	75-300	150-230	250-2000	100-5000	150-230	130-245	400-1600	500-2000	500-5000+
Efficiency	70-92%	60-70%	60-66%	85-90%	75-90%	90%	80-99%	85-99%	97+%
Durability (years)	5-15	5-20	3-15	5-20	15	8-14	15-20	20+	20+
Durability (cycles)	500-1200	1000-2500	200-1500	100-10,000	2000-5000	2500-3000	1,000,000	100,000+	1,000,000+
Capital cost ($/kWh)	200-400	800-1500		600-2500	300-500	100-200	1000-5000	1000-10,000	300-2000
Technology maturity	5	4	4	4	4	4	4	3	3

The PEH system, as previously explained in Chapter 2, generates pulsed energy hence it is necessary to choose a technology that grants the storage of this type of energy. Scrutinizing Table 3.1 it is important to look for technologies that provide a high power density as well as a good cycle life. Lead-acid, Ni-Cd, NiMH, NaS and Zebra batteries have low power density when compared to Li-ion battery, Flywheels, SMES and Supercapacitors. In terms of cycle life, Figure 3.9 helps to better understand the position of each technology.

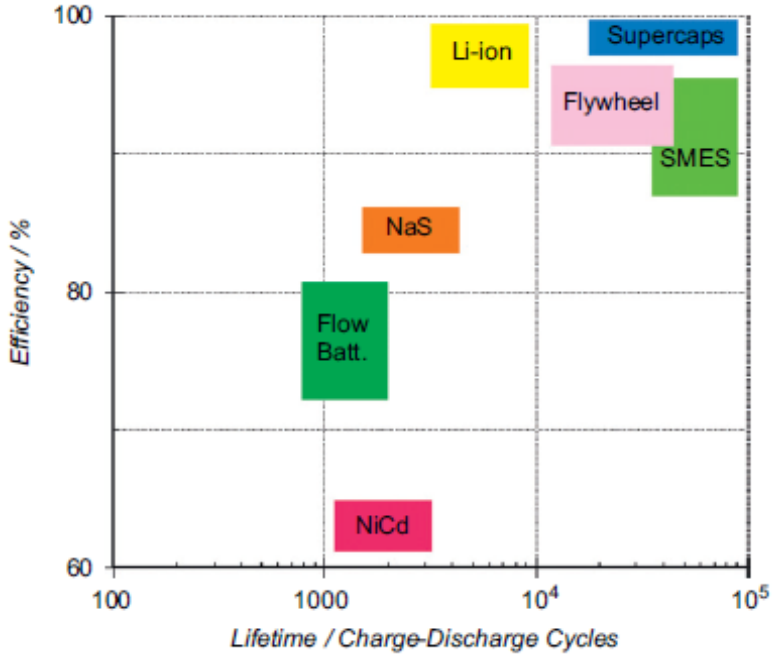

Figure 3.9: Efficiency vs lifetime, source [14]

Together, Table 3.1 and Figure 3.9 lead to the conclusion that the supercapacitor is the technology which best fits storing pulsed energy, being the one with higher power density and higher cycle life combined with a very good efficiency and a reasonable capital cost. Among batteries, clearly Li-ion technology presents the best efficiency and cycle life. Although when compared to flywheels, SMES and supercapacitors fall short in these two characteristics.

The analysis of Table 3.2 shows that, even though perfect for storing pulsed energy, supercapacitors show high self-discharge, making it necessary to combine this technology with a second

Table 3.2: Comparison of storage duration

	Storage duration	
	Self-discharge per day	Suitable storage duration
Li-ion	0.1-0.3%	minutes-days
Flywheels	100%	seconds-minutes
SMES	10-15%	minutes-hours
Supercapacitors	20-40%	seconds-hours

storage stage for storing energy during a long period of time. To overcome the poor energy storing performance of supercapacitors two possible solutions for the second storage level are considered: Li-ion batteries and ultracapacitors.

As said before, ultracapacitors combine the characteristics of EDLCs and Li-ion batteries, presenting high power density as well as good energy-density. Figure 3.10 helps to better understand the position of ultracapacitors (LiCs) in a Ragone plot.

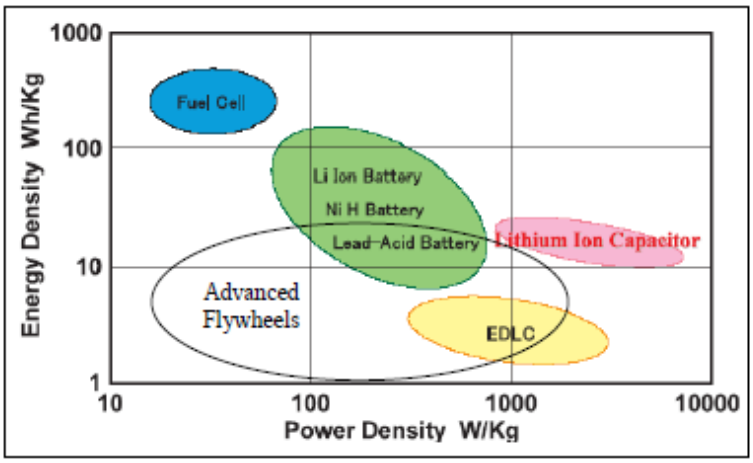

Figure 3.10: Ragone plot, source [17]

Since supercapacitors show a quick discharge time, the second storage stage needs to present a quick response in charging, meaning that the technology to be applied in the second stage requires a high power density. For this particularly reason, ultracapacitors prove to be a suitable technology to be implemented in this storage stage. A third storage stage could be considered with the implementation of Li-ion batteries to obtain a longer storage duration.

Chapter 4

Pavement Energy Harvesting System modelling

4.1 Introduction

The pulsed energy generated by the Pavement Energy Harvesting (PEH) system makes the development of its energy storage a different challenge from the conventional electrical energy generation systems. In Chapter 3 electrical storage system technologies state-of-the-art, electric double layer capacitor (EDLCs), and Lithium-ion capacitors (LiCs), referred here as ultracapacitors, were proven to be the best suitable technologies to meet the requirements of a pulsed energy generation. To develop an efficient and effective storage solution, a model of the PEH system was developed using MATLAB & Simulink. By this mean, supercapacitors (SC) and ultracapacitors (UC) storage systems could be tested and evaluated in an expeditious way.

In this Chapter, several configurations of the PEH system, from the energy generation till the energy storage, are presented and simulated.

4.2 Vehicle-PEH system interaction modelling

As explained in Chapter 2, each PEH module comprises an electro-mechanical system responsible for converting the vertical displacement of the module surface into angular displacement of the generators shafts. This means that the force delivered by a vehicle moving across the module surface induces acceleration on both generators shafts and triggers their rotation.

4.2.1 Vehicle delivered force modelling

While moving across the module surface, vehicles gradually deliver a force to the electro-mechanical system. The maximum value transmitted force depends on the vehicle weight and its

evolution through time depends on the vehicle speed.

$$maxF_{SM2} = \frac{m_v * g}{4} \qquad (\mathrm{N}) \tag{4.1}$$

$$t_1 = \frac{l_m}{s_v} \qquad (\mathrm{s}) \tag{4.2}$$

$$t_2 = \frac{l_{vw}}{s_v} \qquad (\mathrm{s}) \tag{4.3}$$

Assuming the even distribution of the vehicle weight through the four wheels, and since one wheel at a time moves across the module surface, Equation (4.1) defines the maximum force delivered by the vehicle to the PEH module. Equation (4.2) expresses the duration of the contact between the vehicle wheel and the module surface (t_1) relating the vehicle speed (s_v) and the module width (l_m). Once the front wheel passes through the module surface, F_{SM2} becomes zero until the back wheel reaches the module. Once again, F_{SM2} suffers an evolution similar to the one provoked by the front wheel. The time between the crossing of the front and back wheel through the module surface (t_2) is given by Equation (4.3) relating the distance between the two wheels (lvw) and the vehicle speed.

Figure 4.1 depicts the evolution of F_{SM2} considering Equations (4.1) (4.2) and (4.3), and the input data regarding the characteristics of the vehicle and the PEH module is presented in Table 4.1 below.

Table 4.1: F_{SM2} input data

Variable name	Value	Unit
Vehicle class	Light	-
Vehicle weight	1500	(kg)
Vehicle distance between front and back wheels	3.5	(m)
Vehicle speed	40 / 11.1	(km/h)/(m/s)
Module's width	0.35	(m)

4.2.2 Generator's acceleration and speed evolution

The crossing of a vehicle through the PEH module, and consequent force delivered from one to another, induces acceleration on the generator shafts ($\ddot{\theta}_{gen}$) and triggers their rotation. Equation (4.4) expresses the relation between the force F_{SM2} and the acceleration of the generator shaft.

$$\ddot{\theta}_{gen} = \frac{F_{SM2} r_p - (b_{cb} + b_{gen})\dot{\theta}_{gen} - ET}{J_p + J_{sh} + J_{iw} + J_{gen}} \qquad (\mathrm{rad\,s^{-2}}) \tag{4.4}$$

The generator shaft acceleration depends on F_{SM2}, the generator rotation speed ($\dot{\theta}_{gen}$), the electric torque produced by the generator (ET) and several variables referring to the module electro-mechanical system, such as the mechanical system pinion radius (r_p), the mechanical system

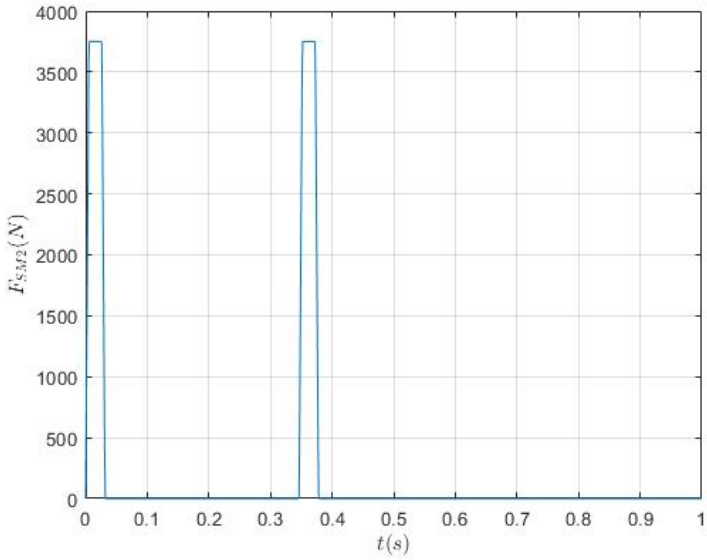

Figure 4.1: Evolution of F_{SM2}

clutch bearing friction coefficient (b_{cb}), the electrical generator friction coefficient (b_{gen}), the moment of inertia of the system pinion (J_p), of the system shaft (J_{sh}), of the inertia wheel (J_{iw}) and of the generator (J_{gen}). The variables values are presented in Table 4.2 concerning the PEH module electro-mechanical system based on the existing PEH module prototype.

Table 4.2: Electro-mechanical system constants values

Variable	**Value**	**Unit**
r_p	0.01275	(m)
b_{cb}	0.002	-
b_{gen}	0.0008	-
J_p	0.000005	(kg.m^2)
J_{sh}	0.0000025	(kg.m^2)
J_{iw}	0.0012	(kg.m^2)
J_{gen}	0.02	(kg.m^2)

4.3 Generator modelling

Each PEH module comprises two eight pole single-phase permanent-magnet alternating current (AC) synchronous generators responsible for converting the mechanical energy delivered into electrical energy. The generator was modeled by the circuit presented in Figure 4.2 according to [18] and [19].

Equation (4.5) expresses the electromagnetic force (E) in relation to the generator rotational speed and the generator constant (k_b). The electric torque (ET) produced by the generator, which opposes to the mechanical system motion, is determined by the product of the current that flows

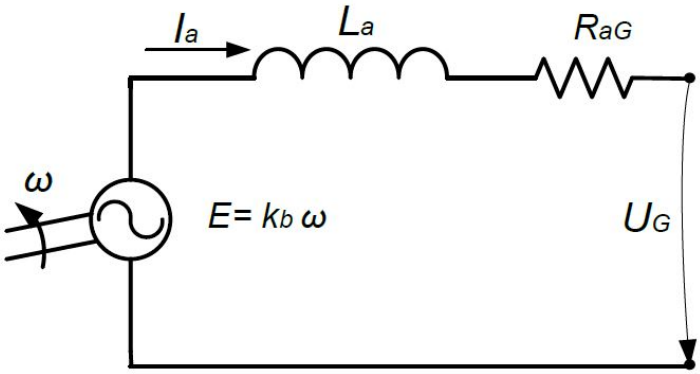

Figure 4.2: Generator electric circuit

to the energy storage (I_{str}) and the generator constant (k_t) through Equation (4.6). The generated current (I_a) and the the terminal voltage (U_G) are obtained directly from the simulation,as well as the generated power (P_G) and energy (E_G).

$$E = k_b \dot{\theta}_{gen} \qquad (\mathrm{V}) \tag{4.5}$$

$$ET = k_t I_{str} \qquad (\mathrm{N\,m}) \tag{4.6}$$

In Figure 4.3 it is presented the circuit used to reproduce the generator model on the Simulink environment. A controlled voltage source is used to define the relation between the generator rotational speed and the electromagnetic force. The required parameters of the PEH module generators are presented in Table 4.3.

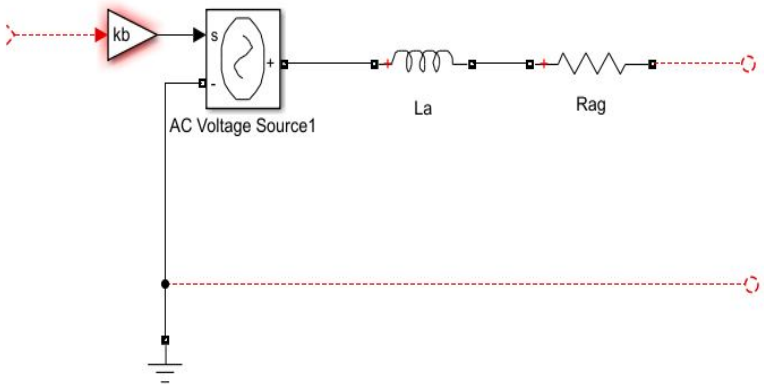

Figure 4.3: Simulink generator model

Table 4.3: Generator model parameters

Variable	Value	Unit
L_a	3.2	(mH)
R_{aG}	1.4	(Ω)
k_b	0.58	-
k_t	0.32	-

4.4 AC-DC Conversion system modelling

To adapt the generated current from alternating current (AC) to direct current (DC) to store the energy produced by the generators, an AC-DC conversion system is implemented. Two possible circuits were studied, modelled and tested in order to find the most efficient and effective solution. Figure 4.4 shows the Simulink model of a single-phase Bridge Rectifier (BR) circuit built according to [20] and Figure 4.5 shows the Simulink model of the Voltage Doubler (VD) circuit built according to [21].

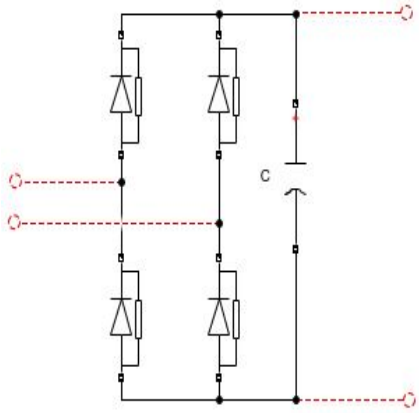

Figure 4.4: Simulink single-phase Bridge Rectifier electric model

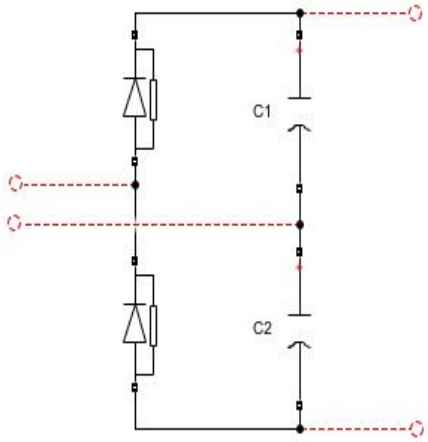

Figure 4.5: Simulink Voltage Doubler electric model

4.5 Energy Storage modelling

Presently (year 2020) different researchers have proposed several EDLC models to handle different purposes, e.g capturing electrical behaviour, thermal behaviour, self-discharge, aging simulation, etc. On one hand simple and explicit models express the overall behaviour of the supercapacitor. On the other hand, more complex models are aimed to a specific behaviour of the EDLC in detail [22][23].

For the electrical behaviour modeling, the one intended in this project, three basic approaches have been presented: a mathematical model, an electric circuit model, and other non-electric circuit models, like artificial neural networking modeling method. Mathematical and non-electric modelling includes complicated computations and depends upon several experimentally identified parameters. Furthermore these types of modelling can not promptly be incorporated into a circuit diagram since they do not commonly present explicit physical meaning[24].

Electric circuit models combine parameterized resitive and capacitive (RC) networks to simulate the electrical behaviour of supercapacitors. With structural simplicity and trustworthy modeling accuracy, electric circuit models are the most frequently used in electrical system behaviour simulations. The electric circuit model accuracy depends on its configurations and the element number. The more complex and sophisticated the circuit, the better the model accuracy[23]. The typical EDLC equivalent circuits models presented in the literature are illustrated in Figure 4.6.

The simplest equivalent circuit model is the RC model depicted in Figure 4.6(a). From the electrical point of view an EDLC can be modelled by an equivalent series resistor (ESR) connected with a capacitor. The capacitor accounts for the capacitance effect and the equivalent series resistor represents the overall resistance[23]. A equivalent parallel resistor (EPR), can be added to account for the self-discharge phenomenon. Due to its extremely large value, the simplified model is

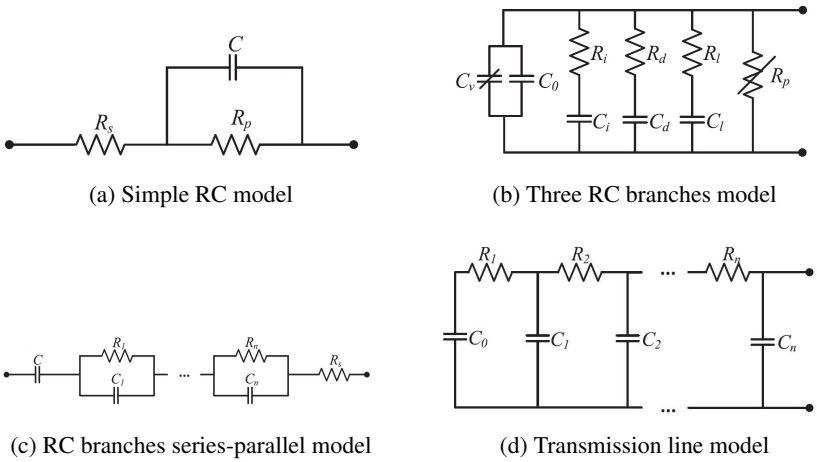

(a) Simple RC model

(b) Three RC branches model

(c) RC branches series-parallel model

(d) Transmission line model

Figure 4.6: EDLC equivalent circuit models, source [23]

more commonly used[25]. The simplicity of the model is its the main advantage, as it is easy to incorporate into a circuit and the simulation process is computationally straightfoward. On the other hand, the Simple RC model fails in capturing the non linear rise and fall of the supercapacitor and can only adequately represent the supercapacitor dynamic behaviour over a time scope of several seconds[24].

Another model presented in the literature is the Three RC Branches model in Figure 4.6(b). This model targets power electronic applications and consists in three RC branches, the immediate branch, the delayed branch and the long term branch. Each branch accounts for the EDLC behaviour on a distinct time-scale through three distinct RC time constants. The immediate branch expresses the charge and discharge behavior in the order of few seconds. The delayed branch expresses the behaviour over the scale of minutes and the long term branch dictates the long term charge and discharge characteristics[23][13]. Similar models were formulated from the Three RC Branches models, including the temperature impact on the model parameters, a variable resistor to represent the self-discharge process and the full-frequency behaviour of the supercapacitor. In [26] a procedure to determine the required model parameters from terminal measurements during a high constant current charging process has been developed.

The EDLC can also be modeled by the RC series-parallel branch model. This model, illustrated in Figure 4.6(c), comprises a series resistor, a bulk capacitor, and, at least, two parallel RC networks. Each parallel RC branch represents the EDLC's pore impedance. The parameters can be obtained with the impedance spectroscopy testing method[24].

Finally, Figure 4.6(d) shows the RC transmission line model. This model is based on Porous Electrode Theory and takes into account dynamic and long time supercapacitor behaviour. This model presents a complex analytical expression hinder its application in simulation. Like the Three RC Branches model, the parameters are obtained from constant current test[24].

Ultracapacitors can also be modelled based on equivalent circuits of serial and parallel combinations of resistors and capacitors to represent its voltage and current characteristics[27]. However,

the ultracapacitors technology is a recent technology and its modelling has not yet been extensively studied[28].

For the purpose of this simulation, both supercapacitors and ultracapacitors were modelled according to the RC simple model. The comparison between the simulation and experimental results in charging and discharging process presented in [24] proves that, even though this model is not the most accurate, the RC Simple model can adequately reflect the supercapacitor dynamic behaviour over a time scope of several seconds. This time scope is enough to understand the supercapacitor response in storing the pulsed energy coming from the PEH system. In addition, this model does not require an experimental procedure method to determine its parameters, since the ESR and capacitance is given by the manufacturer's datasheet. In [29] the RC simple model is used to model ultracapacitors, confirming the proper representation of the ultracapacitor behaviour during charge thus its feasibility to be used in this project.

In [30] a study was conducted to chose the most suitable option to be applied in the energy storage of the PEH system among the supercapacitors and ultracapacitors solutions available. From this study, the Maxwell 16V/ 58F supercapacitor module and JMEnergy 3.8V/3300F ultracapacitor where chosen. The ESR, capacitance value and the voltage operation range, the essential parameters to model and simulate the super and ultracapacitors, are presented in Table 4.4 and the Simulink models are illustrated in Figure 4.7.

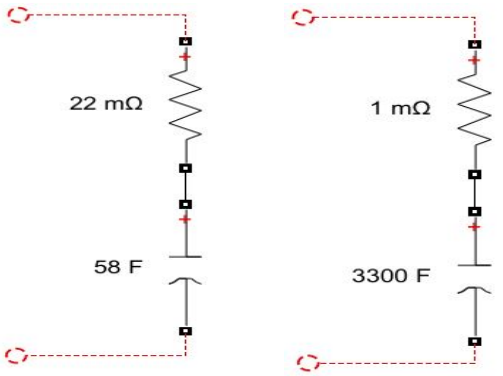

(a) Simulink Supercapacitor model

(b) Simulink Ultracapacitor model

Figure 4.7: Simulation equivalent models

Table 4.4: Supercacitor and Ultracapacitor model parameters

	Supercapacitor	**Ultracapacitor**
Capacitance (F)	58	3300
ESR (mΩ)	22	1
Rated Voltage (V)	0 - 16	2.2 - 3.8

Moreover, an energetic analysis of the energy storage is possible through monitoring the terminal voltage of the supercapacitor or ultracapacitor, resorting to Equation (4.7).

$$E_{str} = \frac{1}{2}CV_{final}^2 - \frac{1}{2}CV_{initial}^2 \qquad (\mathrm{J}) \tag{4.7}$$

4.6 Computational Simulations

A PEH module model was developed in MATLAB & Simulink combining the models presented above. This model aims to simulate the electrical behaviour of one module of the PEH system when a vehicle moves across it and to perform an analysis of the storage system performance.

Considering the input data presented in Table 4.5, several combinations of conversion systems, control mechanism and storage technologies, presented in the above Section, were developed and simulated in order to chose the most efficient and effective one in storing the pulsed electrical energy coming from the PEH module.

Firstly, several system configurations were tested using one supercapacitor module as the energy storage technology. From the result analysis of these configurations, one is elected as the most efficient and then tested using ultracapacitors as the energy storage system.

Afterwards, a configuration involving two modules of the PEH system connected to the same energy storage system is also simulated and analysed.

The simulation outputs are presented as graphic representations of the mechanical quantities of the electro-mechanical system and the evolution of the generator and storage system electric quantities. Conjointly, a table presents numerically the maximum generator rotational speed ($\dot{\theta}_{gen,max}$), the energy production from each one of the two module generator (E_{Gi}), the DC energy supplied to the storage system (E_{DC}) and the stored energy (E_{str}). Moreover, the efficiency of the AC-DC conversion system(η_{AC-DC}), the efficiency of the storage system (η_{str}), and the overall system efficiency (η_{total}), given by Equation (4.8), Equation (4.9) and Equation (4.10) respectively, are presented as well.

$$\eta_{AC-DC} = \frac{E_{DC}}{E_{G1} + E_{G2}} \times 100 \qquad (\%) \tag{4.8}$$

$$\eta_{str} = \frac{E_{str}}{E_{DC}} \times 100 \qquad (\%) \tag{4.9}$$

$$\eta_{total} = \frac{E_{str}}{E_{G1} + E_{G2}} \times 100 \qquad (\%) \tag{4.10}$$

Table 4.5: Simulation input data

	Variable name	**Value**	**Unit**
Vehicle	Vehicle class	Light	-
	m_v	1500	(kg)
	l_{vw}	3.5	(m)
	s_v	40 / 11.1	(km/h)/(m/s)
PEH module	L_a	3.2	(mH)
	R_{aG}	1.4	(Ω)
	k_b	0.58	-
	k_t	0.32	-
	r_p	0.01275	(m)
	b_{cb}	0.002	-
	b_{gen}	0.0008	-
	J_p	0.000005	($kg.m^2$)
	J_{sh}	0.0000025	($kg.m^2$)
	J_{iw}	0.0012	($kg.m^2$)
	J_{gen}	0.02	($kg.m^2$)
	l_m	0.35	(m)
	Initial $\dot{\theta}_{gen}$	0	(rad/s)
Storage system	SC Capacitance	58	(F)
	SC ESR	22	(mΩ)
	SC Initial Voltage	6	(V)
	UC Capacitance	3300	(F)
	UC ESR	1	(mΩ)
	UC Initial Voltage	2.3	(V)

4.6.1 Systems using supercapacitor energy storage system

Firstly, various system configurations are simulated in all of which a supercapacitor module is used as the energy storage system. The simulation results provide the required information to elect the most efficient and effective system configuration.

4.6.1.1 System 1

The first system to be simulated uses a bridge rectifier as the AC-DC conversion circuit. The system Simulink model is depicted in Figure 4.8 and the simulation results are presented in Figure 4.9 and Table 4.6.

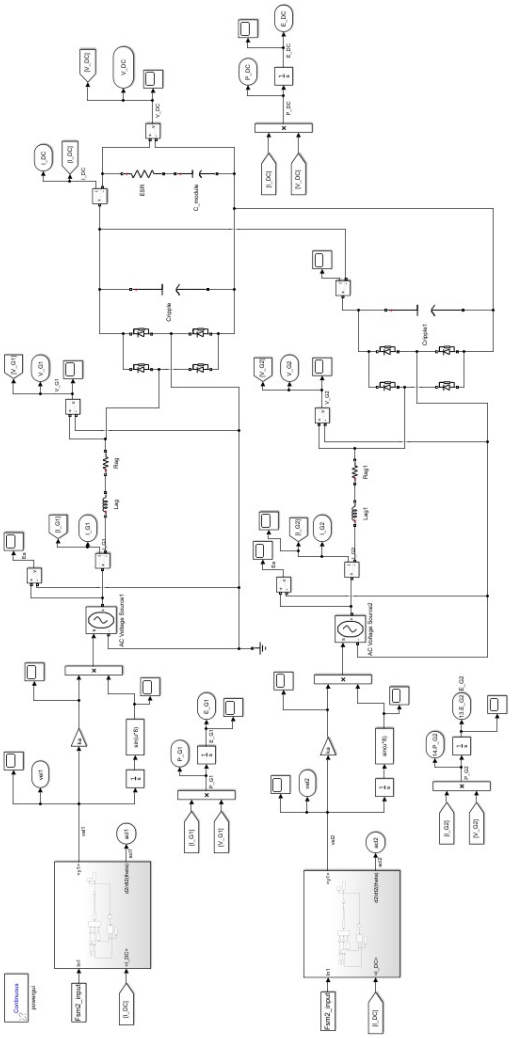

Figure 4.8: System 1 Simulink model

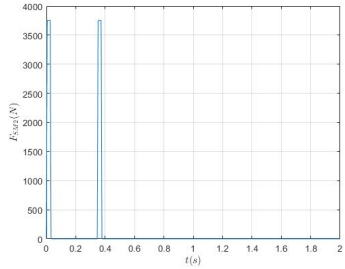

(a) Evolution of F_{SM2}

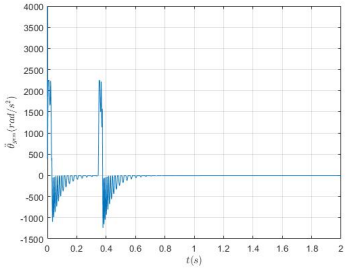

(b) Evolution of the Generator Acceleration

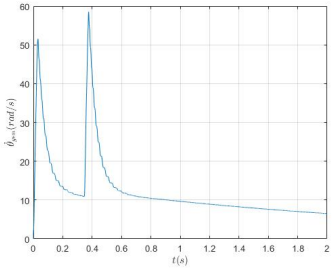

(c) Evolution of the Generator Rotational Speed

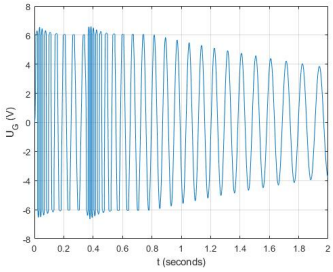

(d) Evolution of the Generator terminal Voltage

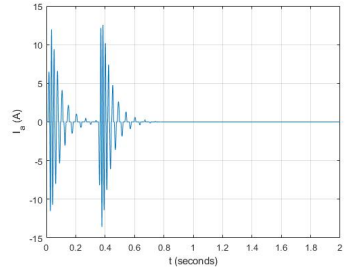

(e) Evolution of the Generator Armature Current

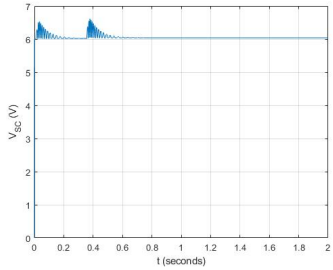

(f) Evolution of the Supercapacitor Terminal Voltage

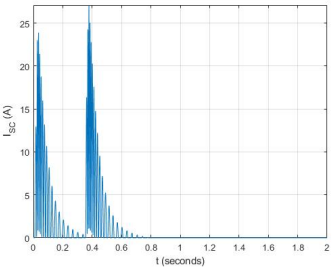

(g) Evolution of the Supercapacitor Current

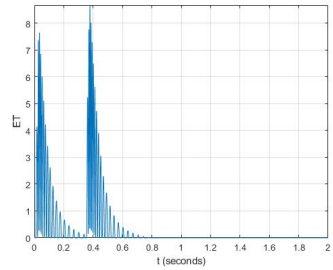

(h) Evolution of the Electric Torque

Figure 4.9: System 1 simulation graphic representations outputs

Table 4.6: System 1 energy and efficiency results

System 1							
$\dot{\theta}_{gen,max}$ **(rad/s)**	E_{G1} **(J)**	E_{G2} **(J)**	E_{DC} **(J)**	E_{str} **(J)**	η_{AC_DC} (%)	η_{str} **(%)**	η_{total} **(%)**
58.51	7.23	7.23	14.31	13.55	98.96	94.73	93.71

4.6.1.2 System 2

Scrutinizing Equation (4.4) and Equation (4.6) one can understand the impact of ET on the acceleration of the generator shaft and its dependence on I_{str}. Aiming for the reduction of this impact a control mechanism was developed. The maximum speed control mechanism (MSCM) is responsible for monitoring the generator rotational speed, and through a switch, connecting the storage system to the generator only when the maximum rotational speed is achieved. By this means the generators can achieve higher terminal voltage at the time of connection to the storage system. System 2 resorts to a bridge rectifier circuit as the AC-DC converter with the additional MSCM. System 2 Simulink model is depicted in Figure 4.10 and the simulation results are presented in Figure 4.11 and Table 4.7.

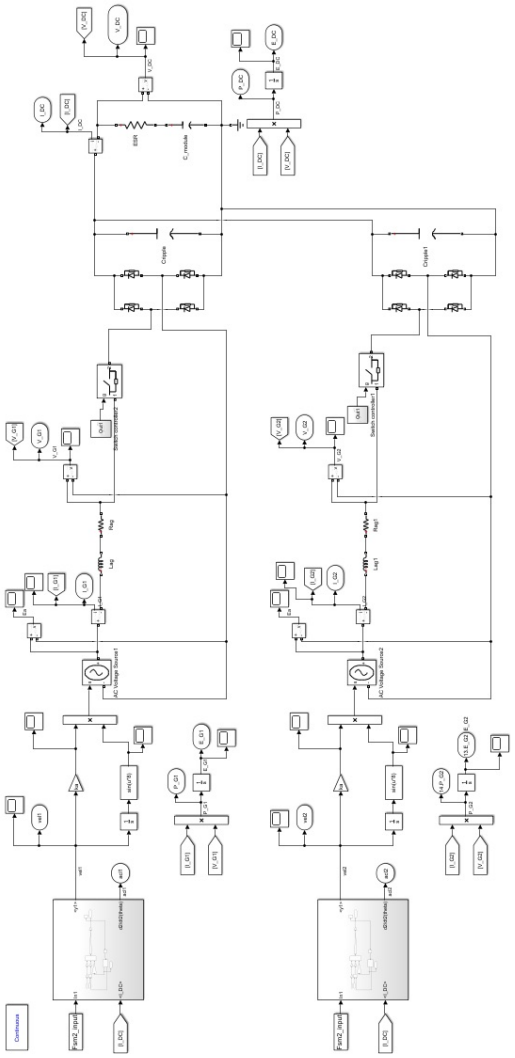

Figure 4.10: System 2 Simulink model

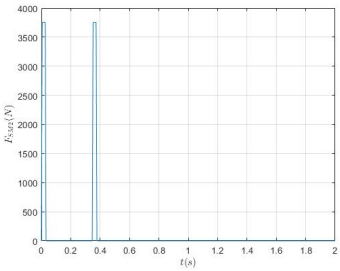

(a) Evolution of F_{SM2}

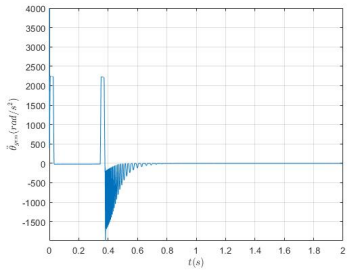

(b) Evolution of the Generator Acceleration

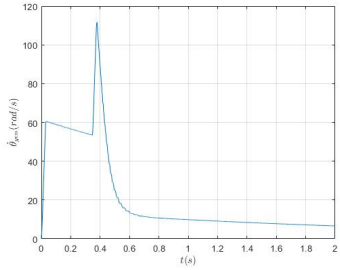

(c) Evolution of the Generator Rotational Speed

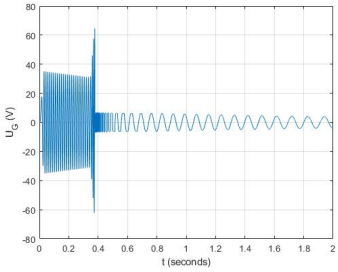

(d) Evolution of the Generator terminal Voltage

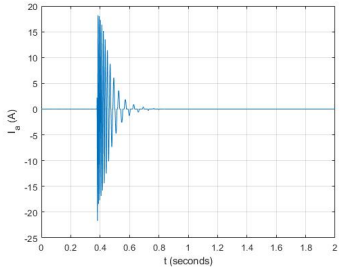

(e) Evolution of the Generator Armature Current

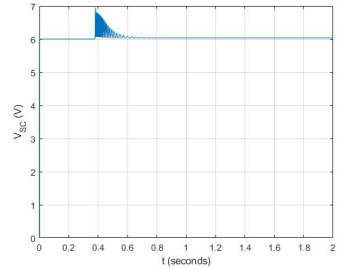

(f) Evolution of the Supercapacitor Terminal Voltage

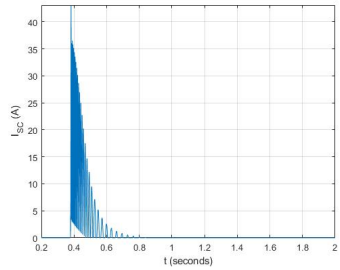

(g) Evolution of the Supercapacitor Current

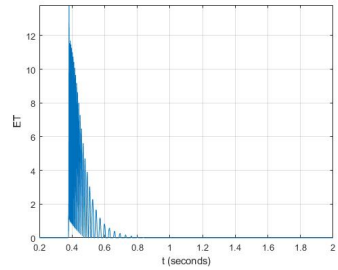

(h) Evolution of the Electric Torque

Figure 4.11: System 2 simulation graphic representations outputs

Table 4.7: System 2 energy and efficiency results

System 2							
$\dot{\theta}_{gen,max}$ **(rad/s)**	E_{G1} **(J)**	E_{G2} **(J)**	E_{DC} **(J)**	E_{str} **(J)**	η_{AC_DC} (%)	η_{str} **(%)**	η_{total} **(%)**
111.57	6.91	6.91	13.63	12.58	98.63	92.27	91.03

4.6.1.3 System 3

System 3, like the aforementioned systems, uses a bridge rectifier circuit as the AC-DC converter and a supercapacitor module as the storage system. One more control mechanism was developed and implemented in this system targeting the reduction of ET in the generator performance. The deceleration tracking control mechanism (DTCM) disconnects the storage system from the generators when their rotation speed starts to decrease. Like MSCM, DTCM allows generators to achieve higher rotational speeds, thus higher terminal voltages. System 3 Simulink model is depicted in Figure 4.12 and the simulation results are presented in Figure 4.13 and Table 4.8.

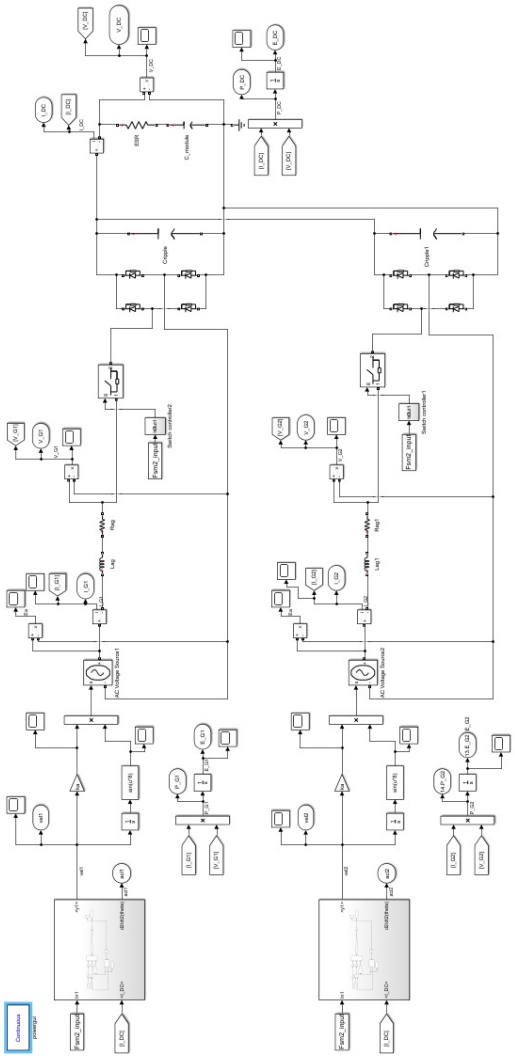

Figure 4.12: System 3 Simulink model

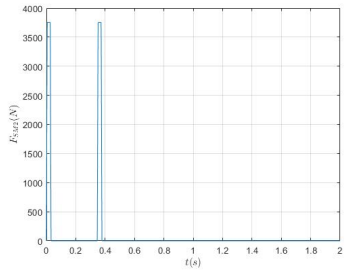

(a) Evolution of F_{SM2}

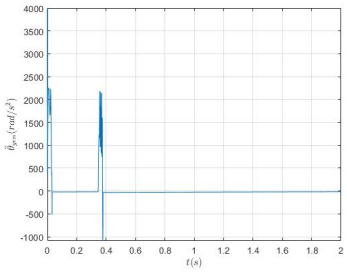

(b) Evolution of the Generator Acceleration

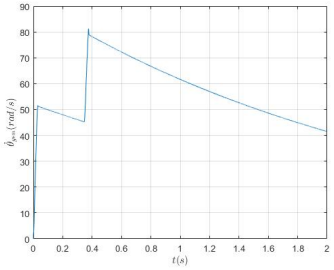

(c) Evolution of the Generator Rotational Speed

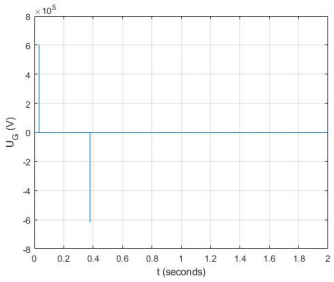

(d) Evolution of the Generator terminal Voltage

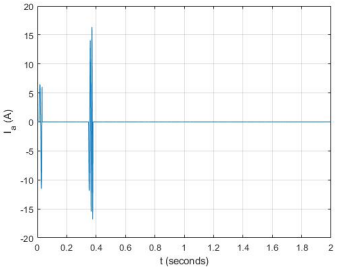

(e) Evolution of the Generator Armature Current

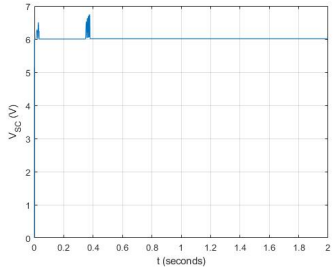

(f) Evolution of the Supercapacitor Terminal Voltage

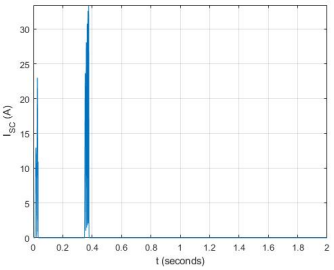

(g) Evolution of the Supercapacitor Current

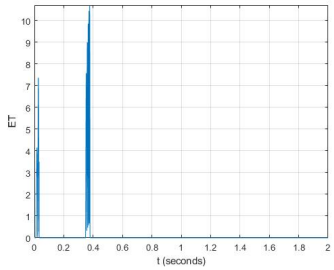

(h) Evolution of the Electric Torque

Figure 4.13: System 3 simulation graphic representations outputs

Table 4.8: System 3 energy and efficiency results

System 3							
$\dot{\theta}_{gen,max}$ **(rad/s)**	E_{G1} **(J)**	E_{G2} **(J)**	E_{DC} **(J)**	E_{str} **(J)**	η_{AC_DC} (%)	η_{str} **(%)**	η_{total} **(%)**
81.22	2.59	2.59	4.74	4.28	91.38	90.30	82.63

4.6.1.4 System 4

Still using the bridge rectifier circuit as the AC-DC converter, System 4 presents a DC-DC boost converter between the the AC-DC converter circuit and the storage system. Once again this simulation aims to analyse the impact on the generators terminal voltage, thus its power and energy generation behaviour. System 4 Simulink model is depicted in Figure 4.14 and the simulation results are presented in Figure 4.15 and Table 4.9.

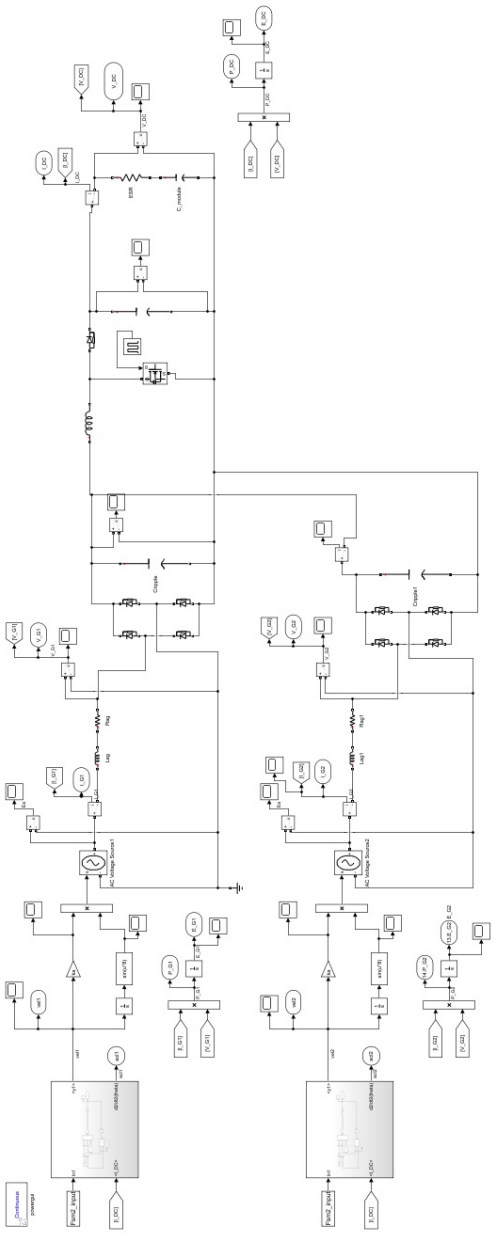

Figure 4.14: System 4 Simulink model

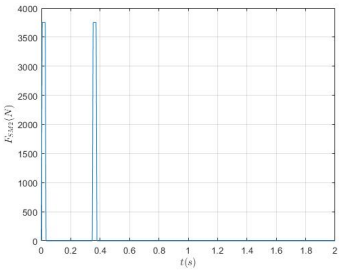

(a) Evolution of F_{SM2}

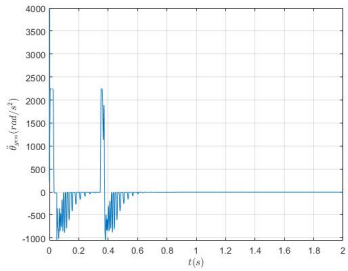

(b) Evolution of the Generator Acceleration

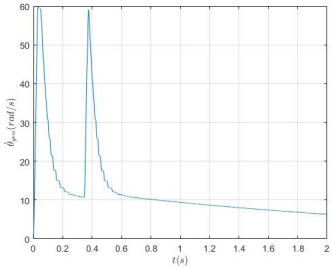

(c) Evolution of the Generator Rotational Speed

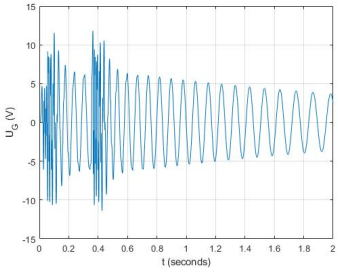

(d) Evolution of the Generator terminal Voltage

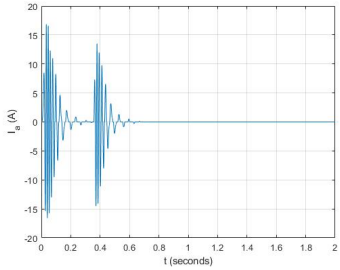

(e) Evolution of the Generator Armature Current

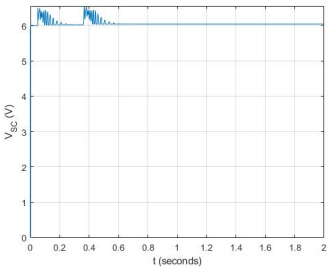

(f) Evolution of the Supercapacitor Terminal Voltage

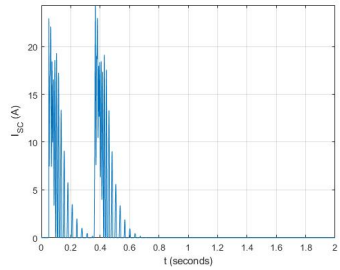

(g) Evolution of the Supercapacitor Current

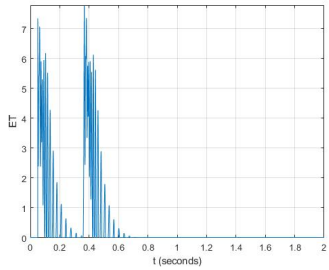

(h) Evolution of the Electric Torque

Figure 4.15: System 4 simulation graphic representations outputs

Table 4.9: System 4 energy and efficiency results

System 4							
$\dot{\theta}_{gen,max}$ **(rad/s)**	E_{G1} **(J)**	E_{G2} **(J)**	E_{DC} **(J)**	E_{str} **(J)**	η_{AC_DC} (%)	η_{str} **(%)**	η_{total} **(%)**
59.66	7.93	7.93	14.29	13.55	90.13	94.84	85.44

4.6.1.5 System 5

System 5 simulates the PEH module system with a Voltage Doubler as the AC-DC conversion circuit. System 5 Simulink model is depicted in Figure 4.16 and Figure 4.17 and Table 4.10 depict the simulation results.

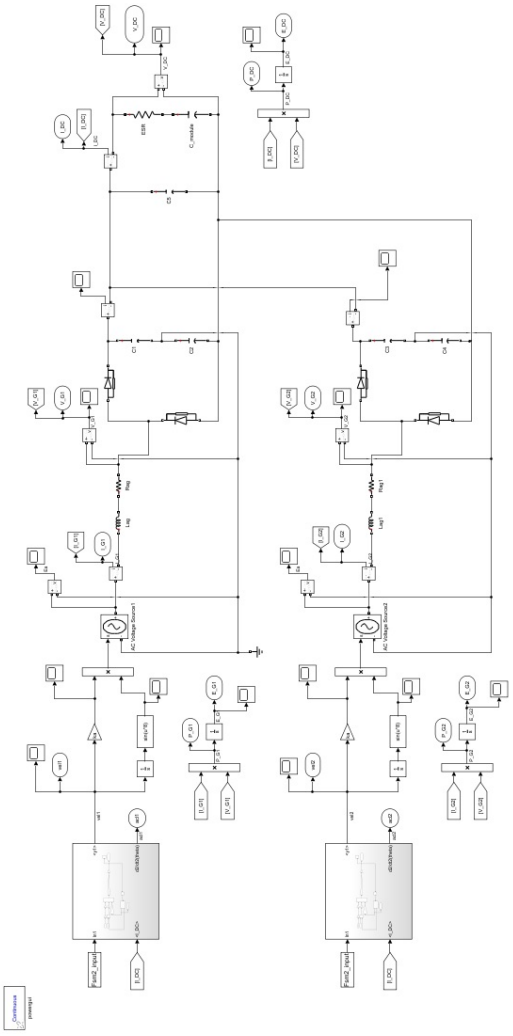

Figure 4.16: System 5 Simulink model

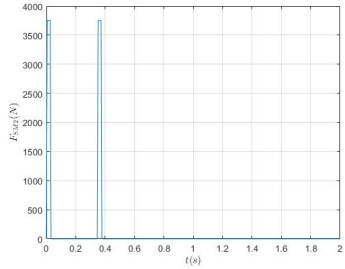

(a) Evolution of F_{SM2}

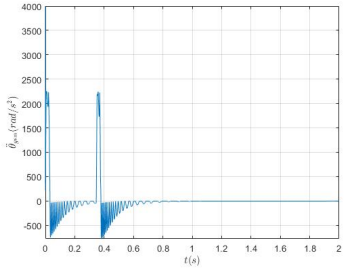

(b) Evolution of the Generator Acceleration

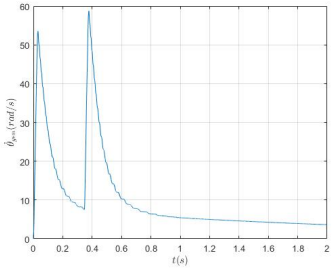

(c) Evolution of the Generator Rotational Speed

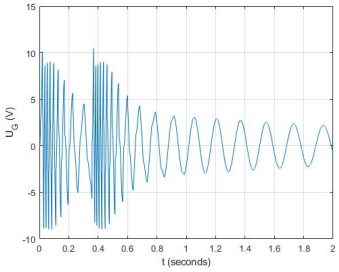

(d) Evolution of the Generator terminal Voltage

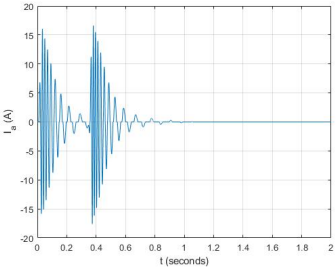

(e) Evolution of the Generator Armature Current

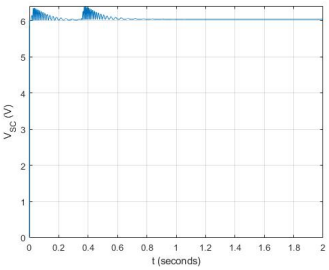

(f) Evolution of the Supercapacitor Terminal Voltage

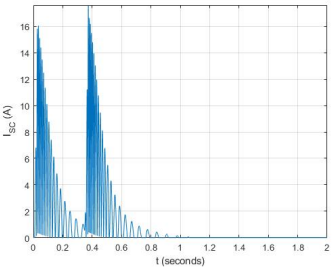

(g) Evolution of the Supercapacitor Current

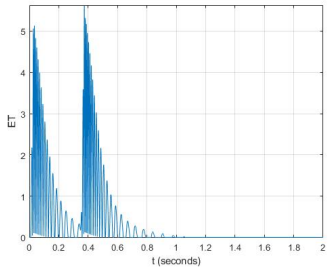

(h) Evolution of the Electric Torque

Figure 4.17: System 5 simulation graphic representations outputs

Table 4.10: System 5 energy and efficiency results

System 5							
$\dot{\theta}_{gen,max}$ **(rad/s)**	E_{G1} **(J)**	E_{G2} **(J)**	E_{DC} **(J)**	E_{str} **(J)**	η_{AC_DC} (%)	η_{str} **(%)**	η_{total} **(%)**
59.76	7.37	7.37	14.74	14.63	99.32	96.72	99.25

4.6.1.6 System 6

Similarly to System 2, System 6 simulates the PEH module system with the MSCM implemented. This system target is to analyse the influence of the MSCM combined with a Voltage Doubler as the AC-DC conversion circuit, using a supercapacitor module as storage system. System 6 Simulink model is depicted in Figure 4.18, and Figure 4.19 and Table 4.11 depict the simulation results.

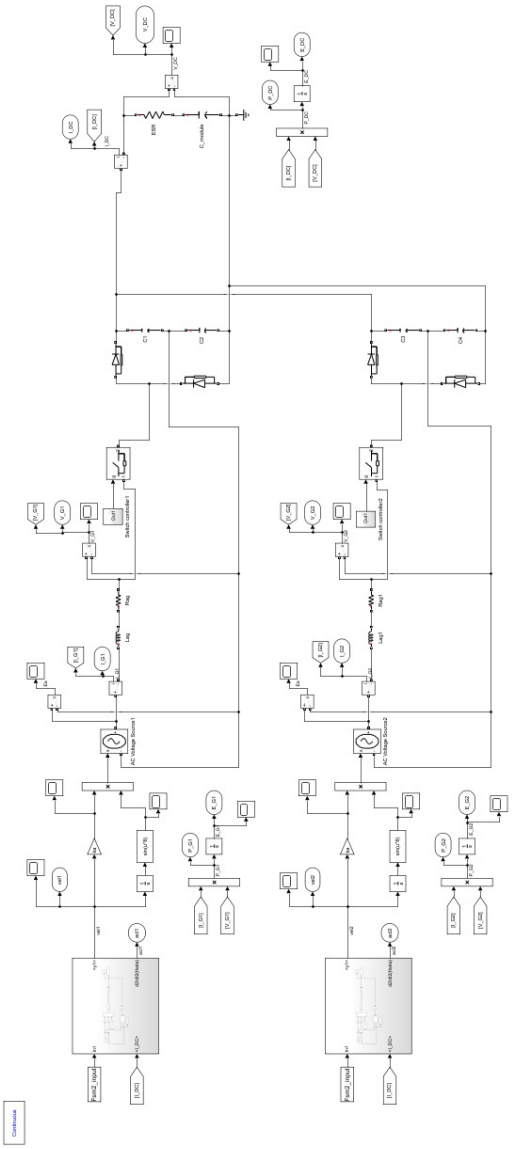

Figure 4.18: System 6 Simulink model

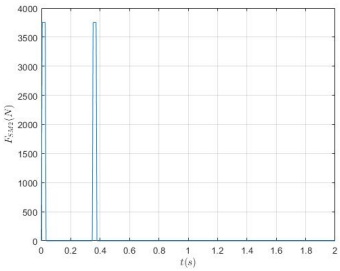

(a) Evolution of F_{SM2}

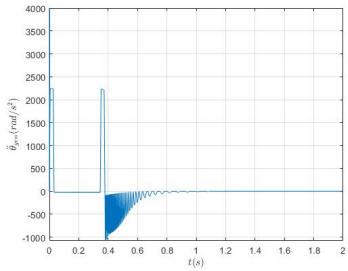

(b) Evolution of the Generator Acceleration

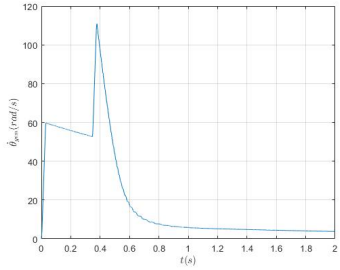

(c) Evolution of the Generator Rotational Speed

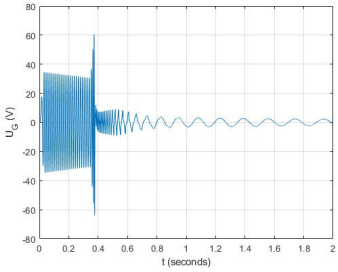

(d) Evolution of the Generator terminal Voltage

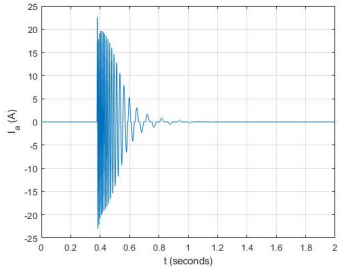

(e) Evolution of the Generator Armature Current

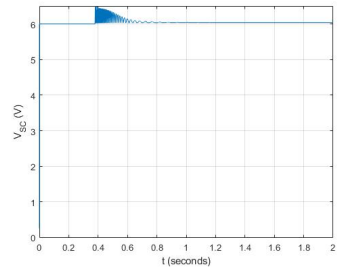

(f) Evolution of the Supercapacitor Terminal Voltage

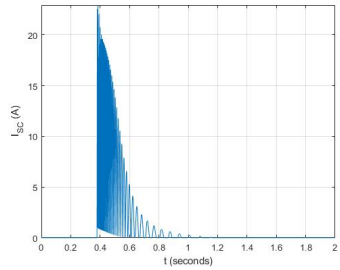

(g) Evolution of the Supercapacitor Current

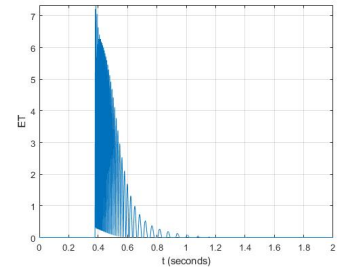

(h) Evolution of the Electric Torque

Figure 4.19: System 6 simulation graphic representations outputs

Table 4.11: System 6 energy and efficiency results

System 6							
$\dot{\theta}_{gen,max}$ **(rad/s)**	E_{G1} **(J)**	E_{G2} **(J)**	E_{DC} **(J)**	E_{str} **(J)**	η_{AC_DC} (%)	η_{str} **(%)**	η_{total} **(%)**
110.80	6.93	6.93	13.67	13.06	98.59	95.53	94.23

4.6.1.7 System 7

Similarly to System 3, System 7 simulates the PEH module system with the DTCM implemented. This system the goal of this system is to analyse the influence of the DTCM combined with a Voltage Doubler as the AC-DC conversion system in the generators energy production, using a supercapacitor module as storage system. System 7 Simulink model is depicted in Figure 4.20 and the simulation results are exhibited in Figure 4.21 and Table 4.12.

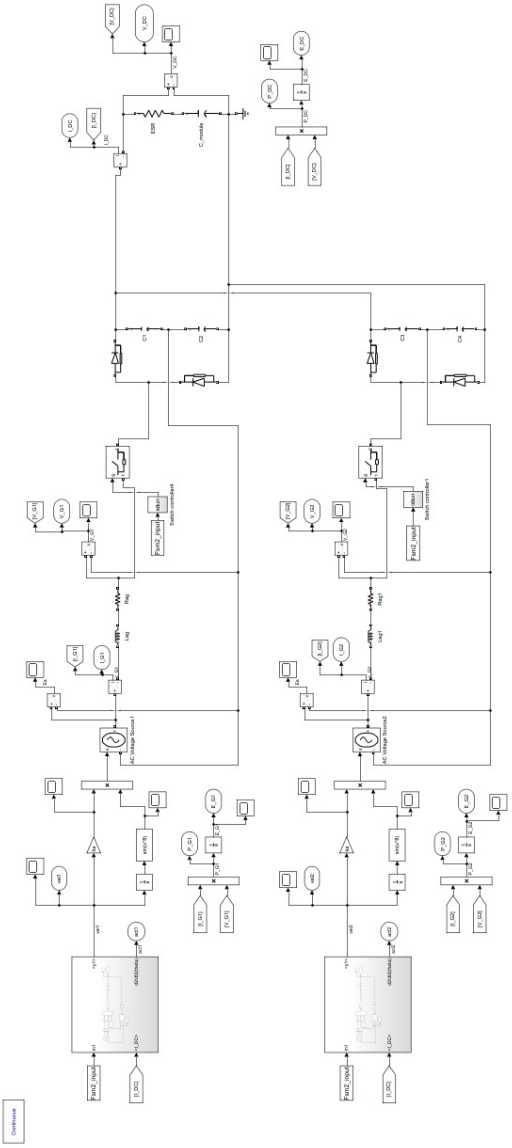

Figure 4.20: System 7 Simulink model

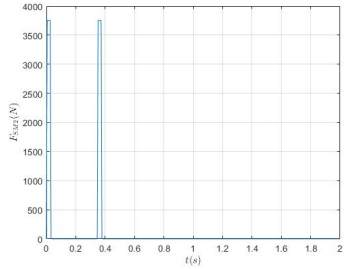

(a) Evolution of F_{SM2}

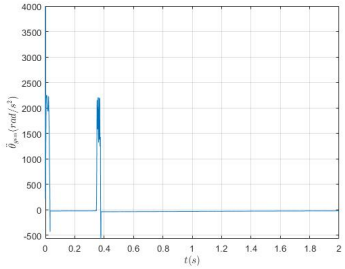

(b) Evolution of the Generator Acceleration

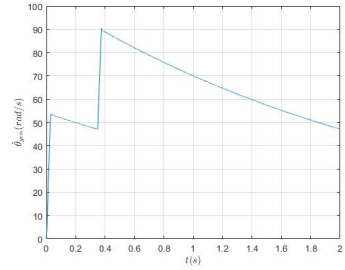

(c) Evolution of the Generator Rotational Speed

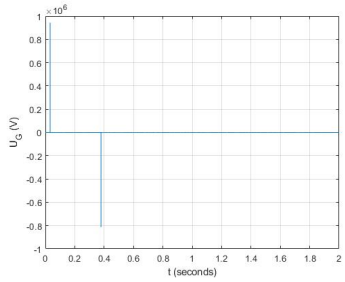

(d) Evolution of the Generator terminal Voltage

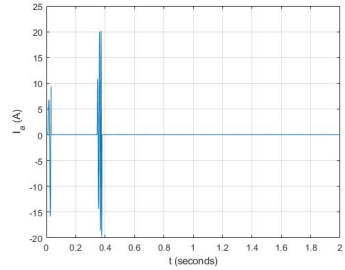

(e) Evolution of the Generator Armature Current

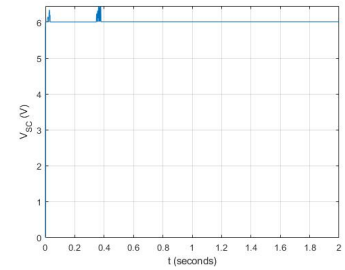

(f) Evolution of the Supercapacitor Terminal Voltage

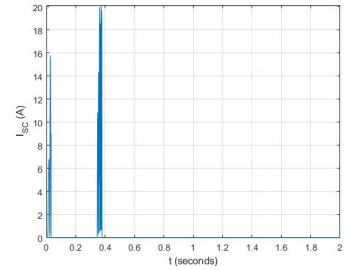

(g) Evolution of the Supercapacitor Current

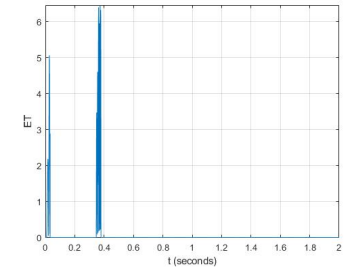

(h) Evolution of the Electric Torque

Figure 4.21: System 7 simulation graphic representations outputs

Table 4.12: System 7 energy and efficiency results

System 7							
$\dot{\theta}_{gen,max}$ **(rad/s)**	E_{G1} **(J)**	E_{G2} **(J)**	E_{DC} **(J)**	E_{str} **(J)**	η_{AC_DC} (%)	η_{str} **(%)**	η_{total} **(%)**
90.53	1.86	1.86	3.02	2.82	80.85	93.50	75.81

4.6.1.8 System 8

Unlike System 6 and 7, System 8 has no control mechanism. Instead, resorting to power electronics, a DC-DC boost converter is implemented between the storage system and the Voltage Doubler circuit. This simulation enables the analysis of the impact of the implementation of the DC-DC boost converter on the generator terminal voltage, thus the impact in the power and energy generation. System 8 Simulink model is depicted in Figure 4.22 and Figure 4.23 and Table 4.13 display the simulation results.

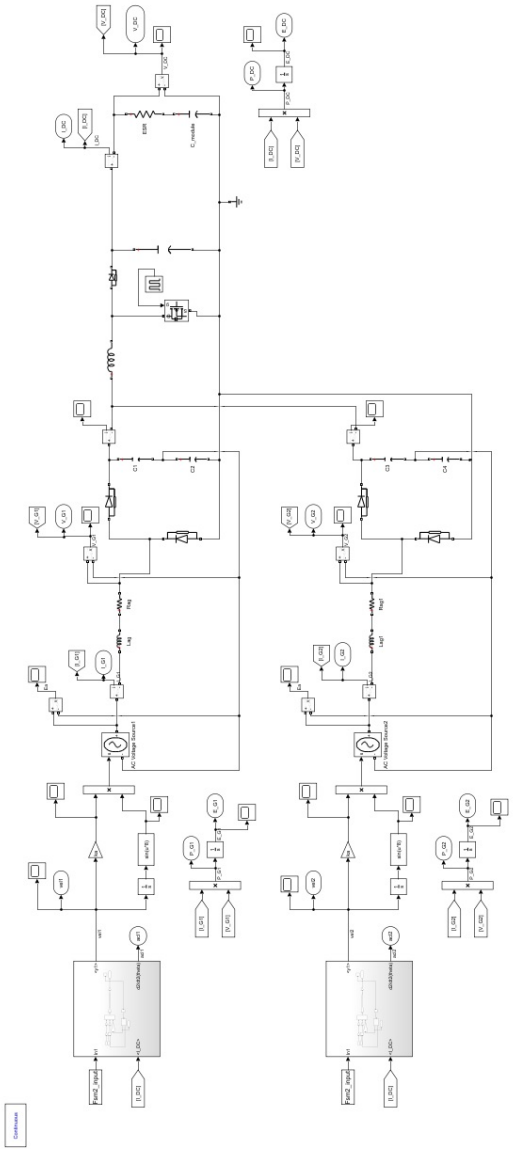

Figure 4.22: System 8 Simulink model

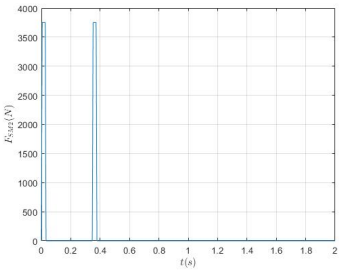

(a) Evolution of F_{SM2}

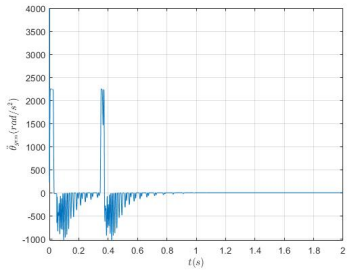

(b) Evolution of the Generator Acceleration

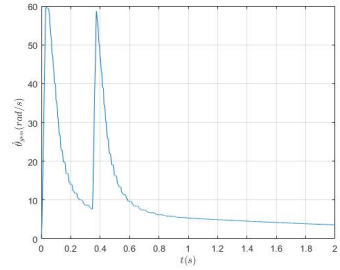

(c) Evolution of the Generator Rotational Speed

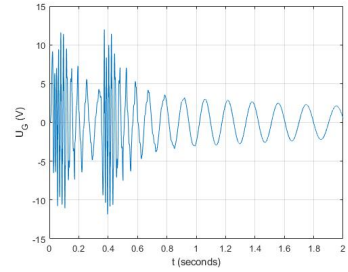

(d) Evolution of the Generator terminal Voltage

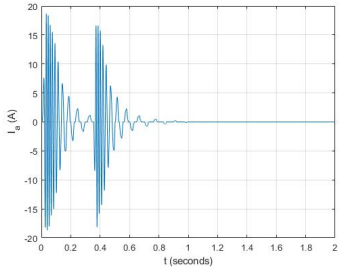

(e) Evolution of the Generator Armature Current

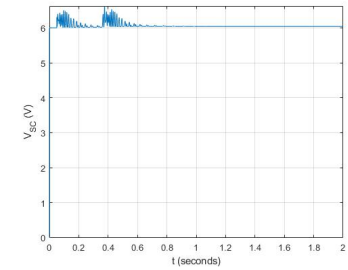

(f) Evolution of the Supercapacitor Terminal Voltage

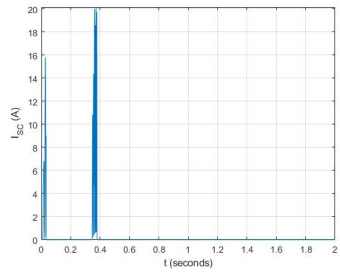

(g) Evolution of the Supercapacitor Current

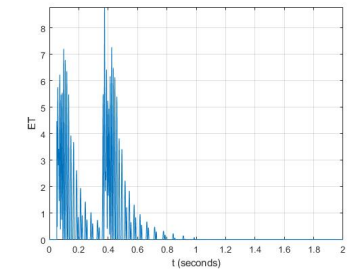

(h) Evolution of the Electric Torque

Figure 4.23: System 8 simulation graphic representations outputs

Table 4.13: System 8 energy and efficiency results

System 8							
$\dot{\theta}_{gen,max}$ **(rad/s)**	E_{G1} **(J)**	E_{G2} **(J)**	E_{DC} **(J)**	E_{str} **(J)**	η_{AC_DC} (%)	η_{str} **(%)**	η_{total} **(%)**
59.66	7.44	7.44	14.79	14.12	99.43	95.47	94.89

4.6.2 Result analysis

Table 4.14 gathers all the energy and efficiency results regarding the various systems configurations using one supercapacitor module as energy storage allowing a more direct comparison of the systems performance.

Table 4.14: Simulation results comparison of systems using supercapacitors

System	$\dot{\theta}_{gen,max}$ **(rad/s)**	E_{G1} **(J)**	E_{G2} **(J)**	E_{DC} **(J)**	E_{str} **(J)**	η_{AC_DC} (%)	η_{str} **(%)**	η_{total} **(%)**
1	58.51	7.23	7.23	14.31	13.55	98.96	94.73	93.71
2	111.57	6.91	6.91	13.63	12.58	98.63	92.27	91.03
3	81.22	2.59	2.59	4.74	4.28	91.38	90.30	82.63
4	59.66	7.93	7.93	14.29	13.55	90.13	94.84	85.44
5	59.76	7.37	7.37	14.74	14.63	99.32	96.72	99.25
6	110.80	6.93	6.93	13.67	13.06	98.59	95.53	94.23
7	90.53	1.86	1.86	3.02	2.82	80.85	93.50	75.81
8	59.66	7.44	7.44	14.79	14.12	99.43	95.47	94.89

After thoroughly analyzing Table 4.14 some conclusions can be drawn.

The storage energy efficiency is greater than 90% for every systems, proving that the supercapacitor module is suitable for storing the pulsed energy coming from the generators.

Scrutinizing Figure 4.9 and Figure 4.17, one can understand that when compared to System 1 that uses only a bridge rectifier AC-DC conversion circuit, System 5, using a voltage doubler as the AC-DC conversion circuit present higher generator terminal voltage and higher generator rotational speed. Table 4.6 and 4.10 prove that System 5 presents higher values of energy generation, as well as higher values of stored energy.

When using MSCM, the storage system is only connected to the generators once the maximum speed is achieved. When scrutinizing Figure 4.11 and Figure 4.19 it is possible to understand that the time corresponding to the connection coincides with the moment when the vehicle back wheel leaves the module surface. That means that the generators only start to charge the supercapacitor module when they are already in the deceleration process. At the moment of the connection the generator terminal voltage assumes the supercapacitor voltage module. Although there is an increase noticed in the charging current of the supercapacitor, it contributes more for the rapidly deceleration of the rotational speed than for the increase of energy delivered to the supercapacitor module.

Figure 4.13 and 4.21 allow to understand how the DTCM works. The storage system begins connected to the generators, and when the generator reaches the maximum speed resultant from the crossing of the front wheel, it is disconnected. Once the back wheel starts crossing the module surface, the storage system is connected again. As the generator reaches the maximum speed resultant from the crossing of the back wheel the storage system is once again disconnected from the generators. As there is no electric torque during the disconnection period, DTCM contributes for achieving higher rotational speeds, but since the storage system connection time is very shortened when comparing to other systems, the energy delivered from the generators to the supercapacitor module is reduced as depicted in Tables 4.8 and 4.12.

Both control mechanisms, MSCM and DTCM, although allowing the achievement of higher generator rotational speeds, fail in increasing the generator energy production. Since the storage system is connected to the generators for a much shorter time period, the energy transmission from the generators to the supercapcitor module in Systems 2, 3, 6 and 7 present low energy production and storage, thus are discarded as suitable options to be implemented.

Systems 4 and 8, with the introduction of a DC-DC boost converter, are the systems with the higher energy generation. By comparing the results of these two systems presented in Table 4.9 and 4.13, System 8 is the one which achieves higher value of stored energy one the supercapacitor module.

Through the result review of the simulations presented above, System 5 is the one chosen to be implemented in the remaining simulations. Even though System 8 presents the higher value of energy generated, System 5 is the one that allows the higher value of energy stored as well as the higher overall efficiency among the systems simulated.

4.6.3 Systems using ultracapacitor energy storage system

The simulation results analysis regarding the systems using a supercapacitor module as energy storage drove to the conclusion that the system that uses the Voltage Doubler as the AC-DC conversion system, and no control mechanism or additional power electronics, is the most effective and efficient solution.

In [30] an experimental validation of the supercapacitor module showed that after 24h a fully charged supercapacitor module loses all the stored energy. This means that when using supercapacitor as storage system, it is required a second stage in the storage system to store energy for longer time periods. In Chapter 3 the comparison of energy storage technologies demonstrated that ultracapacitors present a higher energy density when compared to supercapacitors and high power density as well. Considering the power and energy density characteristics of ultracapacitors, it is studied the possibility of implementing ultracapacitors in the first stage of the energy storage system.

In this way, a new system is developed and simulated, using the same configuration as System 5, but with one or more ultracapacitor cells as the energy storage system.

4.6.3.1 System 9

System 9 simulates the PEH system module with a Voltage Doubler as the AC-DC conversion system and one ultracapacitor cell as the storage system. System 9 Simulink model is depicted in Figure 4.24, and Figure 4.25 and Table 4.15 depict the simulation results.

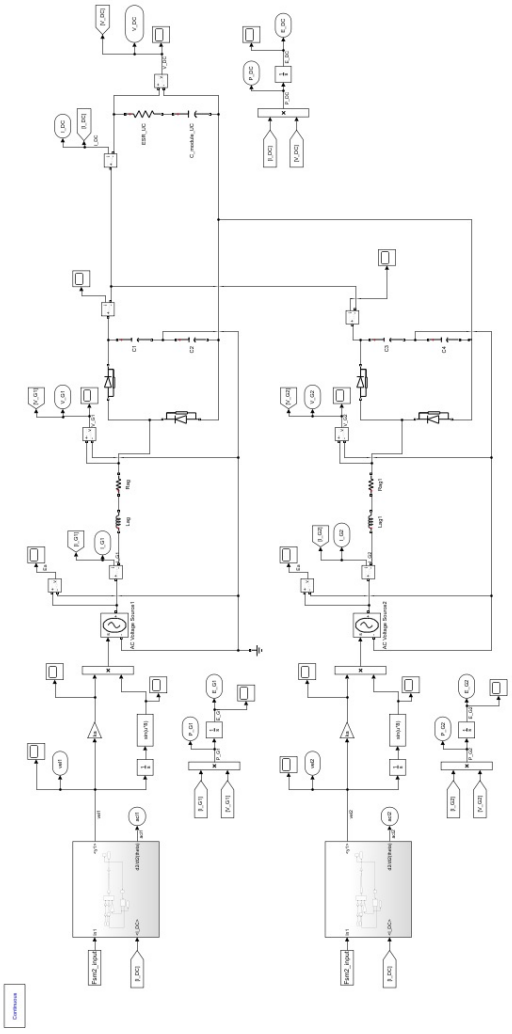

Figure 4.24: System 9 Simulink model

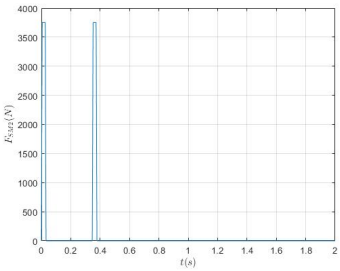

(a) Evolution of F_{SM2}

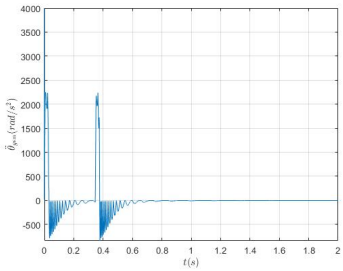

(b) Evolution of the Generator Acceleration

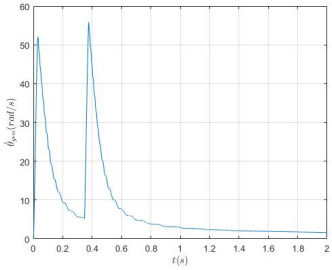

(c) Evolution of the Generator Rotational Speed

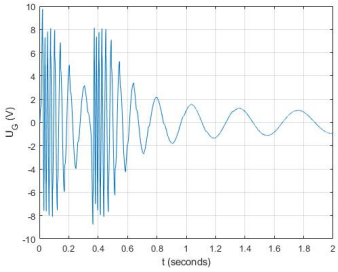

(d) Evolution of the Generator terminal Voltage

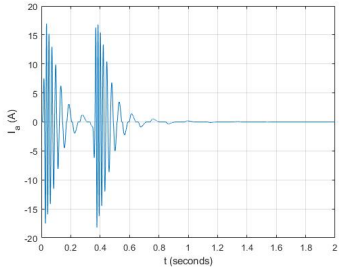

(e) Evolution of the Generator Armature Current

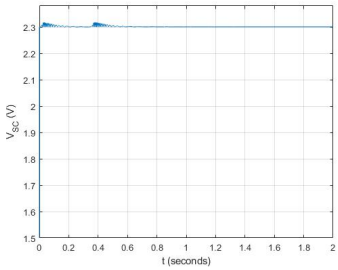

(f) Evolution of the Supercapacitor Terminal Voltage

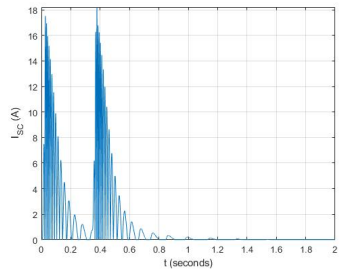

(g) Evolution of the Supercapacitor Current

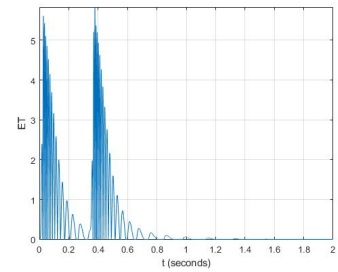

(h) Evolution of the Electric Torque

Figure 4.25: System 9 simulation graphic representations outputs

Table 4.15: System 9 energy and efficiency results

System 9							
$\dot{\theta}_{gen,max}$ **(rad/s)**	E_{G1} **(J)**	E_{G2} **(J)**	E_{DC} **(J)**	E_{str} **(J)**	η_{AC_DC} (%)	η_{str} **(%)**	η_{total} **(%)**
55.76	2.85	2.85	5.65	5.62	99.11	99.48	98.59

4.6.3.2 System 10

The result analysis of the systems using a supercapacitor module as energy storage system led to the conclusion that the terminal voltage of the storage system restrains the energy production of the generators. Since the terminal voltage of the ultracapacitor cell is significantly lower than the one of the supercapacitor module, System 10 aims to simulate the PEH system with multiple series ultracapacitor cells in order to understand the impact of increasing the storage system terminal voltage. Figure 4.26 depicts System 10 with two series ultracapacitor cells as energy storage.

For better understanding, and in order to simplify the energetic analysis, the results using different numbers of series ultracapacitor are presented in Table 4.16

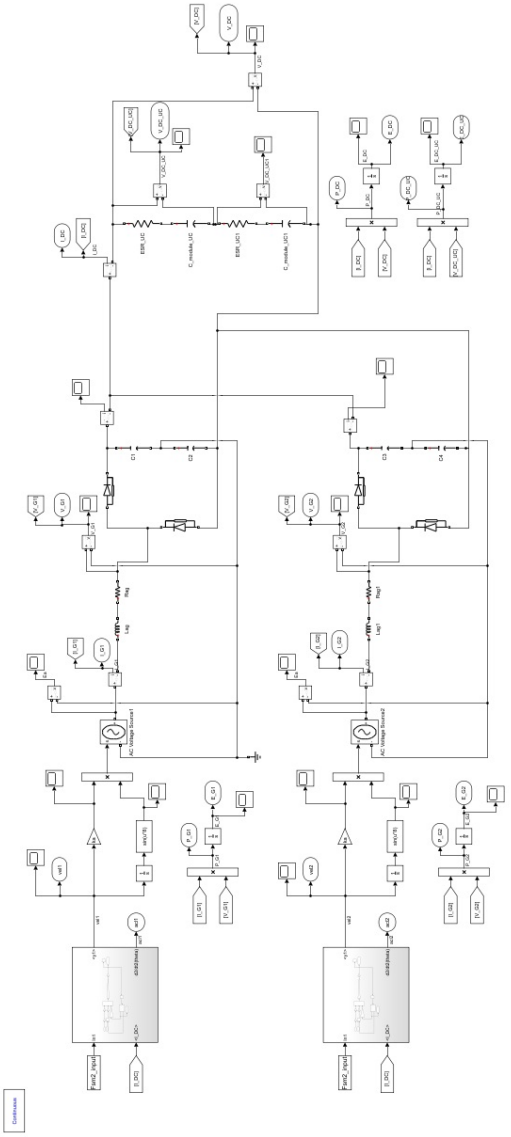

Figure 4.26: System 10 Simulink model

Table 4.16: System 10 energy and efficiency results

System 10								
Series UC	$\dot{\theta}_{gen,max}$ **(rad/s)**	E_{G1} **(J)**	E_{G2} **(J)**	E_{DC} **(J)**	E_{str} **(J)**	η_{AC_DC} (%)	η_{str} **(%)**	η_{total} **(%)**
2	57.41	5.57	5.57	11.06	10.98	99.32	99.33	98.65
3	59.33	8.17	8.17	16.21	16.08	99.28	99.17	98.45
4	62.08	10.64	10.64	21.95	20.88	99.17	98.99	98.17
5	63.77	12.98	12.98	25.71	25.41	99.02	98.82	97.84
6	65.83	15.19	15.19	29.62	30.03	98.85	98.63	97.49
7	68.25	17.27	17.27	34.07	33.54	98.66	98.42	97.10
8	70.71	19.22	19.22	37.84	37.16	98.46	98.21	96.69
10	75.56	22.73	22.73	44.55	43.54	98.00	97.74	95.78

4.6.4 Result analysis

The scrutiny of System 9 and System 10 simulations energy and efficiency results allows for some conclusions to be drawn regarding the use of ultracapacitors as the energy storage system.

Regardless of the number of series ultracapacitors cells, all the systems simulated present energy storage efficiencies greater than 95%. These results ensure that the ultracapacitor cell to be suitable for implementation as the first stage of energy storage.

When using only one ultracapacitor cell as energy storage, Table 4.15 shows that the low terminal voltage of the cell restrains the energy generation. As expected, System 9 presents a low energy production.

Targeting the analysis of the impact of increasing the energy storage system terminal voltage, System 10 was simulated with multiple series ultracapacitors. Table 4.16 shows that the increase of the number of series ultracapacitors cells, thus the increase of the terminal voltage in a proportional way, reflects an increase in energy generation. When compared to System 9, that uses only one ultracapacitor cell, the system that uses ten series ultracapacitors cells notices an increase of around 8 times in the generated and stored energy, whilst the overall efficiency is only 2.81% worse.

4.6.5 Systems using hybrid supercapactior/ultracapacitor energy storage system

The simulation results of the systems using exclusively a supercapacitor module or ultracapacitors cells evidenced the impact of the terminal voltage of the energy storage system in the energy generation and energy storage. Even though higher values of energy generation were achieved using System 10 with multiple series ultracapacitor cells, this solution is expected to be more expensive since it requires more devices. In order to find a solution that could present a substantial energy generation without increasing exponentially the PEH system cost, a hybrid system comprising two stages of energy storage was developed and simulated.

4.6.5.1 System 11

System 11 simulates the PEH system module, using a Voltage Doubler as the AC-DC conversion system and a two stages hybrid energy storage system.

The first stage of the energy storage system is composed of two series supercapacitor modules with a control system that prevents the terminal voltage of each module from being lower than 10V or higher than the rated supercapacitor voltage of 16V. This first stage energy storage system will function as a buffer between the generators and the ultracapacitor cell.

After the supercapacitors modules are charged, these are connected to the ultracapacitor cell and charge it.

For simulation purposes the supercapacitors will only be charged with the generated energy resulting from one vehicle passage, and then immediately discharged to the ultracapacitor cell.

Moreover, in [30] a power circuit to control the charging of an ultracapacitor cell with energy coming from supercapacitors was developed and validated experimentally. From this study

the best solution presented a efficiency of 61% in the energy transmission of the supercapacitor module to the ultracapacitor cell.

With this result it is possible to predict the stored energy on the ultracapacitor cell in the simulation of System 11 resorting to Equation (4.11). This equation relates the stored energy in the two supercapacitor modules (E_{strSC}) and the energy stored in the ultracpacitor cell (E_{strUC}) through the efficiency of the energy transmission process between the two stages of the energy storage system (η_{SC-UC}).

$$E_{strUC} = \eta_{SC-UC} \times E_{strSC} \qquad (\mathrm{J}) \tag{4.11}$$

Figure 4.27 depicts System 11 Simulink model, and Figure 4.28 and Table 4.17 present the simulation results regarding the two stages hybrid storage system.

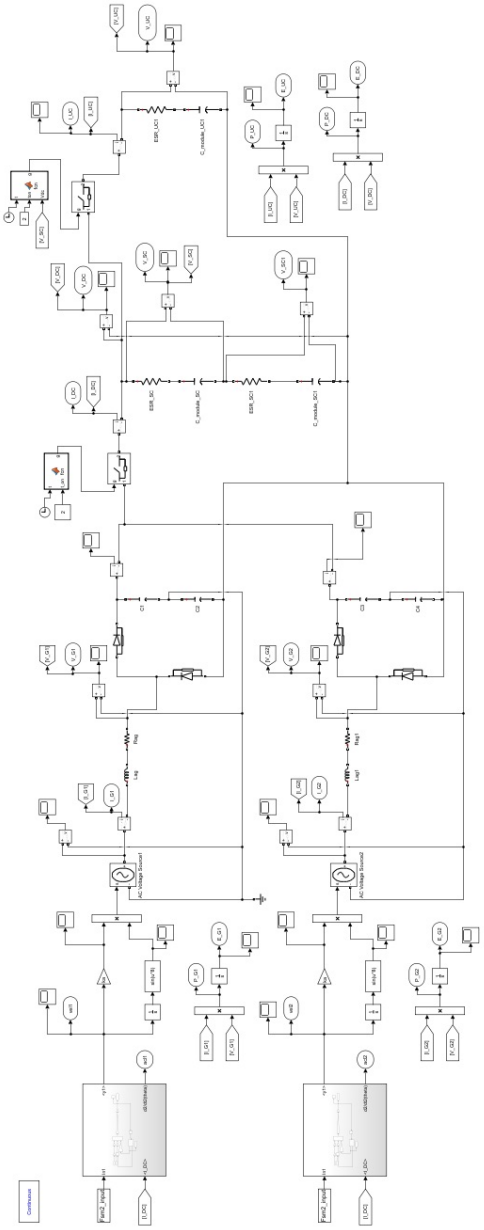

Figure 4.27: System 11 Simulink model

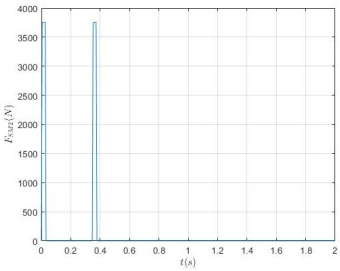

(a) Evolution of F_{SM2}

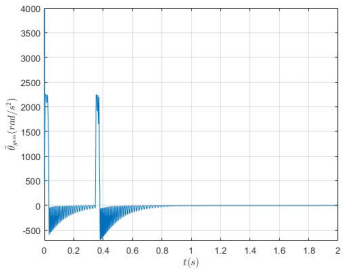

(b) Evolution of the Generator Acceleration

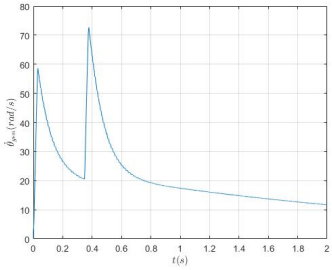

(c) Evolution of the Generator Rotational Speed

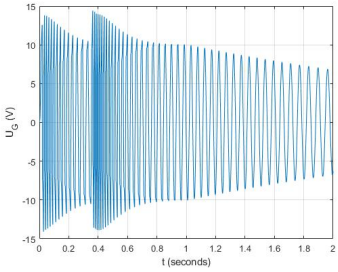

(d) Evolution of the Generator terminal Voltage

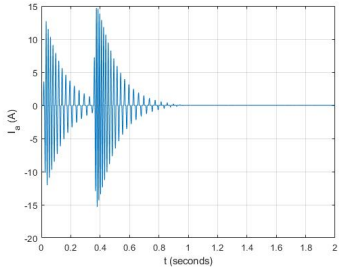

(e) Evolution of the Generator Armature Current

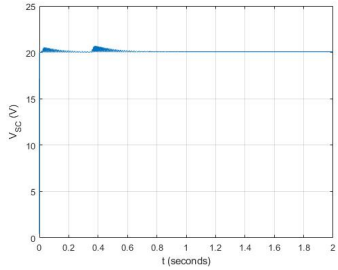

(f) Evolution of the Supercapacitor Terminal Voltage

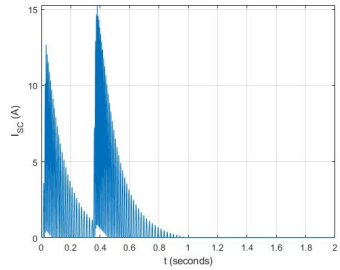

(g) Evolution of the Supercapacitor Current

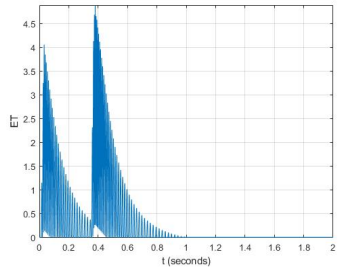

(h) Evolution of the Electric Torque

Figure 4.28: System 11 simulation graphic representations outputs

Table 4.17: System 11 energy and efficiency results

System 11									
$\dot{\theta}_{gen,max}$ **(rad/s)**	E_{G1} **(J)**	E_{G2} **(J)**	E_{DC} **(J)**	E_{strSC} **(J)**	E_{strUC} **(J)**	η_{AC_DC} (%)	η_{strSC} **(%)**	η_{SC-UC} **(%)**	η_{total} **(%)**
72.68	20.75	20.75	40.77	39.50	24.09	98.25	96.89	61	58.07

4.6.6 Result analysis

The System 11 simulations energy and efficiency results allow some conclusions to be drawn regarding the implementation of the hybrid energy storage in the PEH system.

The two series supercapacitor modules allow the increase of the generator terminal voltage, thus the increase in the energy generation. With a control system that prevents the supercapacitor modules terminal voltage from being lower than 10V, it is ensured a higher energy generation than the other systems independently of the state of charge of the energy storage system.

Despite the fact that the low efficiency in the charging of the ultracapacitor cell undermines the overall efficiency of the storage system, System 11 presents a final stage stored energy value similar to the stored energy in System 10 using 5 ultracapacitor cells.

Taking into consideration the final cost of the energy storage, System 11 presents the most cost effective solution to be implemented.

4.6.7 Systems using hybrid supercapactior/ultracapacitor energy storage system for 2 PEH modules

From the simulation of System 11 it was possible to perceive that the implementation of a two stage hybrid energy storage system reflects the best overall performance of the PEH module. Using this system configuration, it is simulated the performance of two PEH system module connected to the same energy storage system.

This simulation focus on understating the impact of a shared energy storage system implementation on the PEH system, since it would allow the reduction of energy storage devices and consequently would represent a more affordable solution.

Two possible systems were simulated: System 12 simulates the connection of two side by side modules to the same energy storage system, and System 13 simulates the connection of two successive modules to the same energy storage system.

For the next simulations it is presented the value of generated energy per module (E_{miG}) instead of the value of generated energy per generator.

4.6.7.1 System 12

System 12 simulates two side by side modules connected to a two stage hybrid energy storage system. This simulation aims to evaluate the performance of the PEH system with the implementation of an energy storage system for the energy coming from two side by side modules.

Standing side by side, both modules are crossed over by the vehicle at the same time, one by the right side wheels and the other by the left side wheels. This means that both modules

experience the same evolution of F_{SM2}, thus the same mechanical and electrical behaviour. Figure 4.29 and Table 4.18 present the System 12 simulation results.

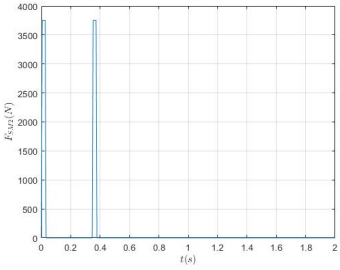

(a) Evolution of F_{SM2}

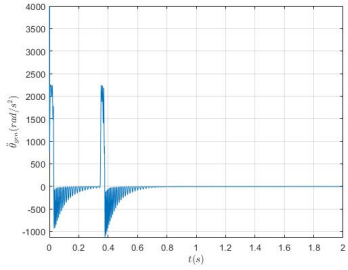

(b) Evolution of the Generator Acceleration

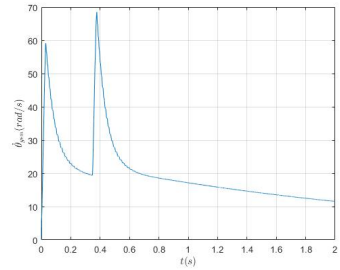

(c) Evolution of the Generator Rotational Speed

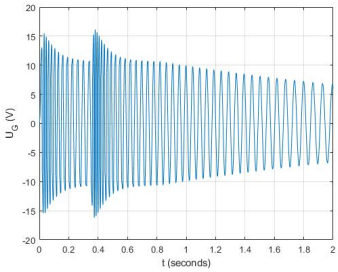

(d) Evolution of the Generator terminal Voltage

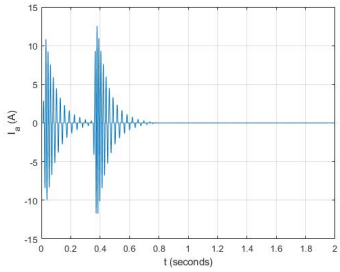

(e) Evolution of the Generator Armature Current

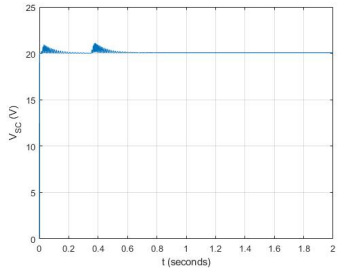

(f) Evolution of the Supercapacitor Terminal Voltage

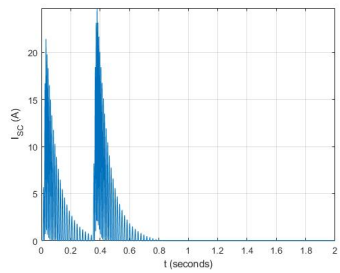

(g) Evolution of the Supercapacitor Current

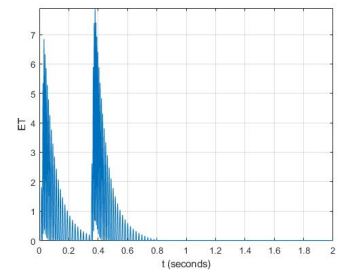

(h) Evolution of the Electric Torque

Figure 4.29: System 12 simulation graphic representations outputs

Table 4.18: System 12 energy and efficiency results

System 12									
$\dot{\theta}_{gen,max}$ **(rad/s)**	E_{m1G} **(J)**	E_{m2G} **(J)**	E_{DC} **(J)**	E_{strSC} **(J)**	E_{strUC} **(J)**	η_{AC_DC} (%)	η_{strSC} **(%)**	η_{SC-UC} **(%)**	η_{total} **(%)**
68.50	26.82	26.82	42.55	40.19	24.52	79.33	94.46	61	45.71

4.6.7.2 System 13

System 13 simulates two successive modules connected to a two stage hybrid energy storage system.

The two successive modules present a dissimilar F_{SM2} evolution and consequently dissimilar mechanical and electrical behaviour. Assuming both modules are installed on the right side of the road lane, the vehicle front right side wheel crosses over the first module, then crosses over the second module. The same happens again with the vehicle back right side wheel. For better understanding of the simulation results, the evolution of the mechanical and electrical quantities of the different modules generators are dissociated in two figures. Figure 4.30 presents the results regarding the first module and Figure 4.31 presents the results regarding the second module. Moreover, the simulation results concerning the evolution of the first stage series supercapacitor modules electrical quantities are presented in Figure 4.32. Finally, Table 4.19 presents the System 13 energy and efficiency simulation results.

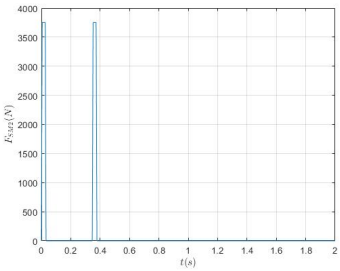

(a) Evolution of F_{SM2}

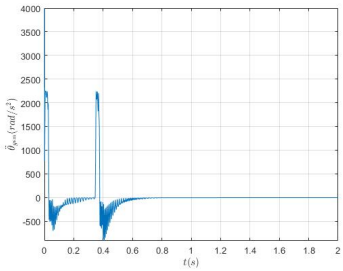

(b) Evolution of the Generator Acceleration

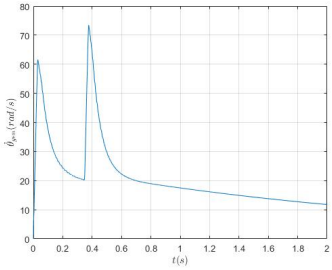

(c) Evolution of the Generator Rotational Speed

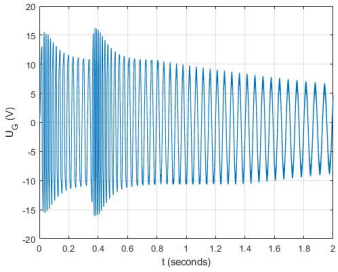

(d) Evolution of the Generator terminal Voltage

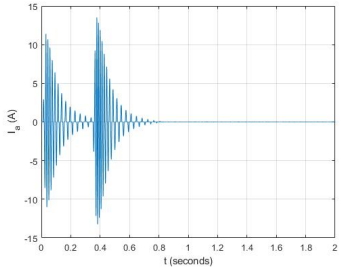

(e) Evolution of the Generator Armature Current

Figure 4.30: System 13 first module simulation graphic representations outputs

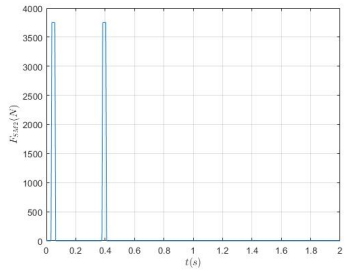

(a) Evolution of F_{SM2}

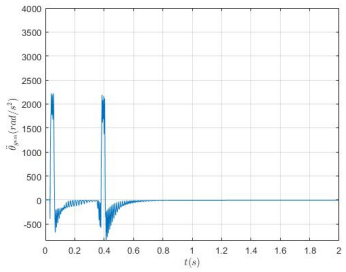

(b) Evolution of the Generator Acceleration

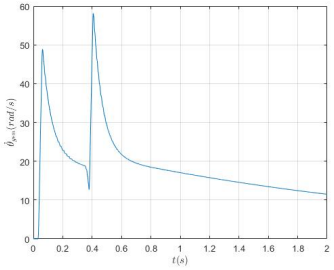

(c) Evolution of the Generator Rotational Speed

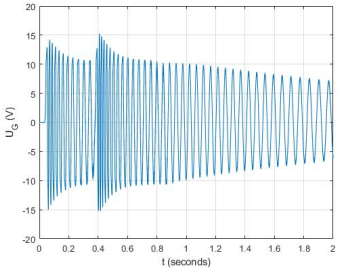

(d) Evolution of the Generator terminal Voltage

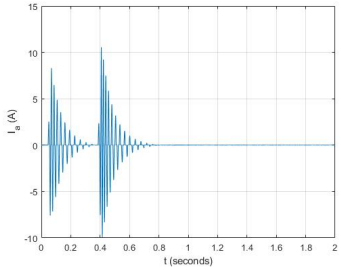

(e) Evolution of the Generator Armature Current

Figure 4.31: System 13 second module simulation graphic representations outputs

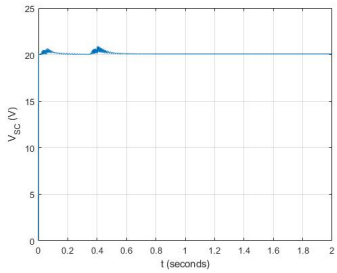

(a) Evolution of the Supercapacitor Terminal Voltage

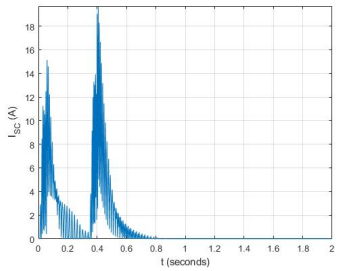

(b) Evolution of the Supercapacitor Current

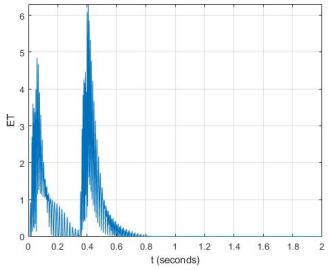

(c) Evolution of the Electric Torque

Figure 4.32: System 13 first stage energy storage simulation graphic representations outputs

Table 4.19: System 13 energy and efficiency results

System 13										
$\dot{\theta}_{1gen,max}$ **(rad/s)**	$\dot{\theta}_{2gen,max}$ **(rad/s)**	E_{m1G} **(J)**	E_{m2G} **(J)**	E_{DC} **(J)**	E_{strSC} **(J)**	E_{strUC} **(J)**	η_{AC_DC} **(%)**	η_{strSC} **(%)**	η_{SC-UC} **(%)**	η_{total} **(%)**
73.45	58.15	34.18	18.56	41.75	39.7	24.22	79.17	95.10	61	45.93

4.6.8 Result analysis

After thoroughly analyzing the simulation results of System 12 and System 13 the following conclusions can be drawn.

When compared to the system that uses the same energy storage system per module, System 12 and 13 present a poorer energy and efficiency performance.

Confronting the simulation results with the ones gathered for System 11, System 12 and 13 present around 50% less energy stored in the second stage of the energy storage system. This means, that in System 11, a single module is capable of storing almost the same amount of energy as two modules in Systems 12 and 13.

4.7 Final Remarks

Throughout this Chapter several possible configurations of the energy storage system were modeled and simulated with the intention to find the configuration that leads to the best energetic performance of the PEH system.

From the simulations with systems using supercapacitors as storage system, one can conclude that this technology is capable of storing the pulsed energy produced by the PEH module. Moreover, these simulations allow the understanding of the impact of the storage system terminal voltage in the overall energetic performance of the PEH module. Even though supercapacitors were proven to be suitable for implementation, the high self discharge rate of this technology obligates a second stage energy storage for storing energy for a longer time period. As anticipated in Chapter 3, due to the considerable fast discharge of supercapacitors, ultracapacitors were elected as the most suitable energy storage technology to be used in the second stage of the storage system.

Since ultracapacitors also present a high power density, the simulation of systems using only ultracapacitors cells as energy storage system was considered before developing a two stage energy storage system. Notwithstanding the capability of storing the pulsed energy coming from the PEH module, due to the low ultracapacitor cell terminal voltage, the PEH modules presented worse energetic values when compared to the ones collected when using supercapacitors. To overcome this voltage restrain, it was then simulated the PEH modules with multiple series ultracapacitor cells. As expected, the increasing number of series ultracapacitor cells reflected the improvement of the PEH module energetic performance. This solution required a considerable number of storage devices as well a charging control system which makes it uneconomically feasible.

Subsequently a two stage hybrid energy storage system, using two series supercapacitor modules as first stage energy storage and a ultracapacitor cell as second and final stage energy storage, was then developed and simulated. As expected, by increasing the generator terminal voltage, with the two series supercapacitor modules, the overall performance of the PEH module noticed improvements.

Finally, two different systems representing the connection of two modules to the same hybrid energy storage systems were simulated. From the simulations results, one can conclude that the connection of two modules to the same energy storage system hinders the overall energetic performance.

From all systems simulations results, it is possible to reckon System 11 as the best configuration for the energy storage system.

Chapter 5

Pavement Energy Harvesting System technical and economic analysis

5.1 Introduction

To prove the feasibility of implementing the Pavement Energy Harvesting (PEH) system it is mandatory to consider, besides all the technical aspects, the economic viability of the technology. In this chapter, a technical and economic analysis is presented in order to evaluate the energy generation of a PEH system during a time period of a year.

5.2 Technical and economic analysis

Since the energy source of the PEH system is the mechanical energy delivered by the vehicles moving through the system, it is important to first consider the traffic data regarding the site of implementation.

The collection of road traffic data on city roads is not yet a common practice, posing difficulties in obtaining accurate data for a specific location. Therefore, in order to carry out a technical and economic analysis, daily traffic estimates will be used for the implementation areas of the system. About 231 000 vehicles enter the city of Porto [31], considering these numbers, for the purpose of this analysis, it is assumed that the road lane where the PEH system is intended to be implemented has a daily traffic of 5% of all the vehicles that enter the city. This means that around 11 550 vehicles cross the PEH system on a daily basis.

The energy generation depends on the type of vehicle that crosses the PEH system. Depending on the weight, different vehicle categories release different amounts of energy to the pavement. For this analysis, and in order to use the results achieved in simulations presented in Chapter 4, only vehicles of Light Class with a weight of 1500 kg are considered.

Since the PEH system under analysis presents a 2×5 layout, the reduction on the vehicle speed is not significant enough to be considered. That means that the force delivered by the vehicle is considered equal for all the 10 modules, meaning that all of the PEH system modules produce

the same amount of energy. From Chapter 4, the PEH module configuration with best energetic performance presented a value of 24.09 J ($6.69 \times 10^{-}3$ Wh) of energy stored per module (E_{str}). Considering that the interval between vehicles is long enough for the generators of each module come to a complete stop, Equation (5.1) translates the total energy stored for the 10 module PEH system ($EPEH$) resulting from the crossing of one vehicle.

$$EPEH = N_{mod} E_{str} \qquad (\text{kWh}) \tag{5.1}$$

To determine the daily amount of stored energy ($DEPEH$), Equation(5.2) relates the average daily traffic (DT) in a proportional way with $EPEH$. Through Equation (5.3) a estimation of the annual stored energy ($AEPEH$) can be forecasted.

$$DEPEH = EPEH \times DT \qquad (\text{kWh}) \tag{5.2}$$

$$AEPEH = DEPEH \times 365 \qquad (\text{kWh}) \tag{5.3}$$

To evaluate the economic value of the energy generated by the PEH system, it is necessary to collect data related with the price of electricity in the intended implementation location. Considering that all the energy produced by the PEH system is used to power electric loads on sight, each kWh produced is equivalent to one less kWh of electricity purchased from the electricity supplier. Equation (5.4) relates the average electrical energy price ($AEEP$) per kWh in a given year and the energy produced in the same time period, expressing the economic value of the energy stored (EVE) by the PEH system. It is considered an average electricity price of 0.2150 €/kWh [32], based on the average electricity price in Portugal in the year of 2019.

$$EVE = AEEP \times AEPEH \qquad (€) \tag{5.4}$$

Table 5.1 presents the results of the technical and economic analyses regarding the implementation of a PEH system.

Table 5.1: Technial and economic analysis results

Variable	**Value**	**Unit**
Average Daily Traffic	11 550	-
Daily PEH system stored energy	0.77	(kWh)
Annual PEH system stored energy	282.10	(kWh)
Average electricity price	0.215	(€/kWh)
EVE	60.65	(€/year)

5.3 Result analysis

From the technical and economic analysis some conclusions regarding the feasibility of implementation of a PEH system can be drawn.

As mentioned before, the collection of road traffic data is still an uncommon practice within cities. The use of more realistic road traffic data of the intended location of the PEH system would help to refine the analysis of the technology implementation viability.

To assess the economic viability of the PEH system, it is important to estimate the payback time period of the technology. To conquer a competitive position within the renewable energy sector market the PEH system should present a payback time period of 5 years. To make this possible the PEH system composed of 10 modules should represent an initial investment of 303.25€, considering the stored energy annual economic value of 60.65€. One can easily conclude that this investment falls short to represent a realistic value.

The economic value of the stored energy by the PEH system depends on two main criteria: the traffic affluence of the installation area and the module energy stored by vehicle. To achieve a more positive economic impact, an increase of the energy stored per module of the PEH system, or a drastic reduction of the technology cost, are required.

The consideration of the possibility of energy injection to the grid, and consequent payment of each kWh injected, could also lever the economic value of the energy stored. Moreover, in the grid injection scenario it could be considered a feed-in tariff contributing for the increasing of the economic value of the energy stored.

Chapter 6

Main Conclusions and Possible Future Works

6.1 Conclusions

The main goal of this work here presented was the development of an energy storage system capable of storing the pulsed energy generated by a Pavement Energy Harvesting (PEH) Solution.

Firstly, it is presented on Chapter 2 a brief explanation of the energy harvesting process of the PEH system, allowing to understand the pulsed nature of the energy generated.

Previous to the development of the energy storage system, a state-of-the-art study on the available energy storage technologies was conducted. From this study, it was possible to identify the most suitable technologies to be implemented as energy storage of the PEH system. Through the comparison of both technical and economic aspects, supercapacitors and ultracapacitors were elected to be the two most promising technologies to meet pulsed energy storage requirements.

Through the medium of the simulation tool developed using MATLAB & Simulink, one PEH system module and several configurations of the energy storage system were modeled and simulated. The modeling of the supercapacitors and ultracapacitors was the first challenge faced when developing the simulation tool for two main reasons:

(i) From the research work conducted on the existing supercapacitor models, the Three RC Branches model was presented as the most trustworthy in representing the supercapacitor behaviour. In order to represent the supercapacitor via this model, it was necessary an experimental procedure to determine the required model parameters from terminal measurements during a high constant current charging process. Due to the pandemic scenario experienced through the realization of this dissertation, and consequent obligation to work remotely, it was not possible to experimentally collect these parameters and the model chosen to be implemented in the simulation was the Simple RC model, since its required parameters could be obtained from the supercapacitor datasheet and no experimental procedure would be required.

(ii) The simulations using supercapacitors as energy storage system allowed to understand how the energy storage terminal voltage restrained the generator voltage, thus the energy generation. Since the terminal voltage of the energy storage system depends on its state of charge, the challenge was to develop a solution to overcome this restriction and consequently increase the energy generation.

By comparing the different systems simulation results, it was possible to understand that the energy storage system that lead to the most effective and efficient results is the two stage hybrid energy storage system. This system, presented in System 11, combines a two series supercapacitor modules as first energy storage stage and a ultracapacitor cell as second energy storage stage. The configuration of this energy storage system allows to dissociate the final energy storage system terminal voltage from the generator terminal voltage and by these means to increase the generators energy delivery.

Lastly, considering the chosen energy storage in Chapter 4 a technical and economic analysis was conducted to evaluate the economic viability of the implementation of a 10 module PEH system.

This analysis allowed to conclude that the PEH system stored energy is inherently related with the energy generation of each module and with the road traffic. The road lane daily traffic considered in the technical and economic analysis was based on a low percentage of the average number of vehicles entering the city of Porto per day, meaning that the PEH system energy stored values achieved are related to its implementation in a busy road lane within a city. Even though high daily road traffic was considered, the still poor energetic performance of the PEH system hinders its economic viability. One can conclude that, in order to improve the economic viability of the PEH system, efforts must be targeted to improve the energetic performance of each PEH module. This improvement can be achieved by increasing the vehicle mechanical energy harvesting or by increasing the conversion efficiency of the mechanical into electrical energy.

The work here developed made it possible to understand that the PEH system, although a promising renewable energy generation technology, requires further developments in increasing the system energetic performance in order to achieve more advantageously economic viability and to conquer a place on the renewable energy sector market.

6.2 Future works

After concluding this study, four subjects are suggested for future developments.

(i) The first suggestion dwells in replacing the supercapacitor Simple RC model used in the simulation for the Three RC Branches model. This model will more accurately represent the supercapacitor behaviour over a longer time span when compared to the simple RC model.

(ii) The second one consists in developing a more efficient power electronics circuit between the first and second stage storage in System 11. By improving the charge of the second stage

energy storage utracapacitor cell, more energy can be stored in this final energy storage stage. A more efficient power electronics would allow the increase of the overall system efficiency thus increasing the stored energy.

(iii) In third place, in order to confirm the models trustworthiness in representing the actual behaviour of the PEH system, it is also suggested an experimental validation of the simulation results.

(iv) Finally the development of a simulation model for an entire PEH system is suggested. By including more modules and a road traffic input, an entire PEH system simulation would help to achieve a more accurate technical and economic analysis.

References

[1] Francisco Duarte and Adelino Ferreira. Energy harvesting on road pavements: State of the art. *Proceedings of Institution of Civil Engineers: Energy*, 169(2):79–90, may 2016. doi:10.1680/jener.15.00005.

[2] Energy Harvesting: Solar, Wind, and Ocean Energy Conversion Systems - Alireza Khaligh, Omer C. Onar.

[3] Shashank Priya and Daniel J. Inman. *Energy harvesting technologies*. Springer US, 2009. doi:10.1007/978-0-387-76464-1.

[4] Tom J. Kázmierski and Steve Beeby. *Energy harvesting systems: Principles, modeling and applications*. Springer New York, 2011. doi:10.1007/978-1-4419-7566-9.

[5] Francisco João Anastácio Duarte. Pavement Energy Harvesting System to Convert Vehicles Kinetic Energy into Electricity. mar 2018.

[6] Haisheng Chen, Thang Ngoc Cong, Wei Yang, Chunqing Tan, Yongliang Li, and Yulong Ding. Progress in electrical energy storage system: A critical review, mar 2009. doi:10.1016/j.pnsc.2008.07.014.

[7] Massoud Pedram, Naehyuck Chang, Younghyun Kim, and Yanzhi Wang. Hybrid electrical energy storage systems. In *Proceedings of the International Symposium on Low Power Electronics and Design*, pages 363–368, New York, New York, USA, 2010. ACM Press. URL: http://portal.acm.org/citation.cfm?doid=1840845.1840924, doi:10.1145/1840845.1840924.

[8] Helder Lopes Ferreira, Raquel Garde, Gianluca Fulli, Wil Kling, and Joao Pecas Lopes. Characterisation of electrical energy storage technologies. *Energy*, 53:288–298, may 2013. doi:10.1016/j.energy.2013.02.037.

[9] Chris Bullough, Christoph Gatzen, Christoph Jakiel, Martin Koller, Andreas Nowi, and Stefan Zunft. Advanced Adiabatic Compressed Air Energy Storage for the Integration of Wind Energy. Technical report, 2004.

[10] John R. Sears. Tex: The next generation of energy storage technology. In *INTELEC, International Telecommunications Energy Conference (Proceedings)*, pages 218–222, 2004. doi:10.1109/intlec.2004.1401469.

[11] Ioannis Hadjipaschalis, Andreas Poullikkas, and Venizelos Efthimiou. Overview of current and future energy storage technologies for electric power applications, aug 2009. doi:10.1016/j.rser.2008.09.028.

[12] Katerina E. Aifantis, Stephen A. Hackney, and R. Vasant Kumar, editors. *High Energy Density Lithium Batteries*. Wiley, apr 2010. URL: https://onlinelibrary.wiley.com/doi/book/10.1002/9783527630011, doi:10.1002/9783527630011.

[13] Yi Cheng Zhang, Li Wei, Xiaojun Shen, and Haiquan Liang. Study of Supercapacitor in the Application of Power Electronics. Technical report.

[14] Peter J. Hall and Euan J. Bain. Energy-storage technologies and electricity generation. *Energy Policy*, 36(12):4352–4355, dec 2008. URL: https://linkinghub.elsevier.com/retrieve/pii/S0301421508004497, doi:10.1016/j.enpol.2008.09.037.

[15] Patrice Simon and Yury Gogotsi. Materials for electrochemical capacitors, nov 2008. doi:10.1038/nmat2297.

[16] Ander González, Eider Goikolea, Jon Andoni Barrena, and Roman Mysyk. Review on supercapacitors: Technologies and materials, may 2016. doi:10.1016/j.rser.2015.12.249.

[17] Raymond B. Sepe, Anton Steyerl, and Steven P. Bastien. Lithium-ion supercapacitors for pulsed power applications. In *IEEE Energy Conversion Congress and Exposition: Energy Conversion Innovation for a Clean Energy Future, ECCE 2011, Proceedings*, pages 1813–1818, 2011. doi:10.1109/ECCE.2011.6064005.

[18] Stephen J Chapman and Bae Systems Australia. Electric Machinery and Power System Fundamentals First Edition. Technical report, 2002.

[19] K M Vishnu Murthy and Giriraj Lane. *Computer-Aided Design of Electrical Machines SSP BS Publications === 4-4-309*. 2008. URL: www.bspublications.net.

[20] Ned Mohan, Tore M. Undeland, and William P. Robbins. *Power Electronics. Converters, Applications and Design*. John Wiley and Sons, Inc, third edition, 2003.

[21] By Joseph M Beck and Senior Applications Engineer. Application Note Vishay General Semiconductor Using Rectifiers in Voltage Multiplier Circuits Vishay General Semiconductor. 2:1477–1480, 2013.

[22] C. Fărcaş, D. Petreuş, I. Ciocan, and N. Palaghiţă. Modeling and simulation of supercapacitors. In *SIITME 2009 - 15th International Symposium for Design and Technology of Electronics Packages*, pages 195–200, 2009. doi:10.1109/SIITME.2009.5407373.

[23] Lei Zhang, Xiaosong Hu, Zhenpo Wang, Fengchun Sun, and David G. Dorrell. A review of supercapacitor modeling, estimation, and applications: A control/management perspective, jan 2018. doi:10.1016/j.rser.2017.05.283.

[24] Lisheng Shi and M. L. Crow. Comparison of ultracapacitor electric circuit models. In *IEEE Power and Energy Society 2008 General Meeting: Conversion and Delivery of Electrical Energy in the 21st Century, PES*, 2008. doi:10.1109/PES.2008.4596576.

[25] L. Palma. Analysis of supercapacitor connection to PV power conditioning systems for improoved performance. In *5th International Conference on Clean Electrical Power: Renewable Energy Resources Impact, ICCEP 2015*, pages 198–203. Institute of Electrical and Electronics Engineers Inc., aug 2015. doi:10.1109/ICCEP.2015.7177623.

[26] Luis Zubieta and Richard Bonert. Characterization of double-layer capacitors for power electronics applications. *IEEE Transactions on Industry Applications*, 36(1):199–205, jan 2000. doi:10.1109/28.821816.

[27] Goran Mandic, Adel Nasiri, Ehsan Ghotbi, and Eduard Muljadi. Lithium-ion capacitor energy storage integrated with variable speed wind turbines for power smoothing. *IEEE Journal of Emerging and Selected Topics in Power Electronics*, 1(4):287–295, dec 2013. doi:10.1109/JESTPE.2013.2284356.

[28] Simone Barcellona, Flavio Ciccarelli, Diego Iannuzzi, and Luigi Piegari. Modeling and parameter identification of lithium-ion capacitor modules. *IEEE Transactions on Sustainable Energy*, 5(3):785–794, 2014. doi:10.1109/TSTE.2014.2301950.

[29] N. El Ghossein, A. Sari, and P. Venet. Interpretation of the Particularities of Lithium-Ion Capacitors and Development of a Simple Circuit Model. In *2016 IEEE Vehicle Power and Propulsion Conference, VPPC 2016 - Proceedings*. Institute of Electrical and Electronics Engineers Inc., dec 2016. doi:10.1109/VPPC.2016.7791712.

[30] Manuel Marco Soares. Conceção de um sistema de eletrónica de potência para armazenamento de energia pulsada em estágios de super e ultracondensadores, feb 2020.

[31] Mais de meio milhãoo de carros entope o Porto todos os dias - JN. URL: https://www.jn.pt/local/noticias/porto/porto/mais-de-meio-milhao-de-carros-entope-o-porto-todos-os-dias-11460350.html.

[32] PORDATA - Preços da electricidade para utilizadores domésticos e industriais (Euro/ECU). URL: https://www.pordata.pt/Europa/Pre{ç}os+da+electricidade+para+utilizadores+dom{é}sticos+e+industriais+(Euro+ECU)-1477.